Developments, ideas, and evaluations based upon Reissner's Mixed Variational Theorem in the modeling of multilayered plates and shells

Erasmo Carrera

Department of Aeronautics and Aerospace Engineering, Politecnico di Torino, Corso Duca degli Abruzzi 24, 10129 Torino, Italy; carrera@polito.it

This review article is devoted to the use of the Reissner Mixed Variational Theorem (RMVT) forward two-dimensional modeling of flat and curved, multilayer structures. A thorough review of the literature involving the use in the modeling of multilayered plates and shells using RMVT is also presented. In the first part, the paper overviews relevant key points that should be taken into account for an accurate description of strain and stress fields in multilayered plate and shell analysis. It is then shown that RMVT has been originated in view of the fulfillment of such key points, herein referred to as C^0-Requirements (zig-zag form of the displacement fields in the thickness direction and continuity of transverse normal and shear stresses at each layer interface). Classical variational statements are used to introduce Reissner's Theorem. In the second part, the paper presents various ways in which RMVT can be used to develop plate and shell theories in a systematic manner. The so called layer-wise and equivalent single layer variable description are considered. Both strong and weak (finite element) forms of governing equations have been derived. A Weak Form of Hooke's Law (WFHL), is also discussed as an idea to eliminate transverse stress variables leading to standard classical models with only displacement unknowns. Two appendices display details of governing equations related to multilayered doubly curved shells and to finite element matrices of multilayered plates. A third part reviews the works that have appeared in literature which make use of RMVT. Mainly papers on multilayered plate and shell modelings have been addressed. The final part of the paper is devoted to giving an overview with selected results of numerical performance that can be acquired by RMVT applications; extensive comparison to elasticity solutions and to other significant analyses, based on classical and refined approaches, are given. It is concluded that Reissner's Mixed Theorem should be considered as a natural tool for multilayered structure analyses; it plays a similar role to that of the Principle of Virtual Displacement in the analysis of isotropic single-layer structures. This review article includes 119 references. [DOI: 10.1115/1.1385512]

1 INTRODUCTION

The literature of the last 15 year shows that *Reissner's Mixed Variational Theorem (RMVT)* has played a significant role toward a better understanding of the mechanical behavior of multilayered structures. This mixed theorem was proposed by the late Professor Reissner in a few articles that appeared in the middle 1980s [1–3]. An introduction to RMVT could best be made by quoting those words that Professor Reissner used in the abstract of his own article [3].

> *We are concerned in this paper with the derivation of a two dimensional system of shell equations by means of the direct methods of the calculus of variations, for an elastic layer the material of which is non-uniform in the thickness direction. We have on earlier occasions considered this problem for transversely isotropic layers with uniform material properties in the thickness direction, by means of classical variational theorem [4], as well as by means of the variational theorem for displacement and stresses [5,6].*
>
> *We now consider the problem of a non-uniform shell, in particular the problem of a laminated shell, as the problem of a three-dimensional anisotropic elastic layer, through the use of a variational equation which has recently been established for displacements and transverse stresses [1,2]. In connection with this equation, we note in particular that with its use we avoid the necessity of making approximations for stresses which may be discontinuous functions of the thickness coordinate, because of the material property discontinuities, while retaining the capability of using approximate expressions for stresses which must be continuous in the thickness direction.*

It clearly appears from Reissner's words that RMVT is at the same time an extension and a particular case of known varia-

ASME Reprint No AMR $24.00
Appl Mech Rev vol 54, no 4, July 2001

tional principles: RMVT is in fact something more than displacement formulations and something less than a full mixed principle. It is a tool especially useful for layered structure analysis; as a main task RMVT requires (or permits) transverse shear and normal stress assumptions to fulfill interface continuity. This review article is devoted to the use of RMVT as a variational tool to analyze multilayered plate and shell structures. The aims and scope of this paper are listed below.

1) To discuss the necessary prerequisites, herein referred to as C_z^0-Requirements, for an accurate description of the response of multilayered structures and their relationship to RMVT (Sections 2 and 3).
2) To present the ways in which RMVT can be used as a tool to formulate the theories for plates and shells, including finite element applications (Sections 4 and Appendices A and B).
3) To present a so-called Weak Form of Hooke's Law (WFHL) (Section 5) as a manner of expressing transverse stress variables in terms of the displacement ones.
4) To give a literature overview of technical papers in which RMVT has been employed (Section 6).
5) To show with the help of published and a few new numerical evaluations, that RMVT is a valuable tool for analyzing global and local behavior of multilayered plates and shells (Section 7).

It is also the author's aim, through the present article, to honor the late Professor Eric Reissner whose valuable works have contributed to a better understanding of the behavior of plate and shell structures over the last century. By anticipating a conclusion of the present work, the author believes that Reissner's Mixed Theorem represents a *natural* tool to analyze multilayered structures.

2 MODELINGS OF MULTILAYERED STRUCTURES

2.1 C_z^0-Requirements

Multilayered structures are increasingly used in aerospace structures, ships, as well as in automotive vehicles. Examples of multilayered anisotropic structures are sandwich constructions, composite structures made of orthotropic laminae, layered structures made of different isotropic layers (such as those employed for thermal protection), as well as intelligent structures embedding piezo-layers. Examples are given in Fig. 1. Mostly plate and shell geometries are addressed in this paper. In these cases multilayered structures are made up by a certain number of layers N_l, that are supposed to be perfectly bonded together and which can be made of isotropic, orthotropic, as well as anisotropic materials. The geometry and notation of shell cases are depicted in Fig. 2. Curvilinear triorthogonal coordinate systems α-β-z in each k-layer are used for the shell cases while the corresponding Cartesian coordinates x-y-z are used for plates. These two systems are used without distinction in this paper; in a few cases both of them are denoted without distinction by numbers 1-2-3.

As far as two dimensional modeling is concerned, the main task of multilayered constructions is related to the possibility of exhibiting different mechanical-physical properties in the thickness direction. Such a peculiarity is herein referred to as *Transverse Anisotropy (TA)*. In addition, anisotropic multilayered structures often exhibit both higher transverse shear and transverse normal flexibilities, with respect to in-plane deformability, than traditional isotropic one-layered ones. This is herein referred to as *High Transverse Deformability (HTD)*. For instance, laminated structures made of advanced composite materials presently used in aerospace structures could exhibit high values of orthotropic Young's moduli ratios ($E_L/E_T = E_L/E_z = 5 \sim 40$, where L denotes the fiber directions, while T and z are two directions orthogonal to L) and the low transverse shear moduli ratios ($G_{LT}/E_T \approx G_{TT}/E_T = 1/10 \sim 1/200$) leading to higher transverse shear and transverse normal stress deformabilities than in isotropic cases.

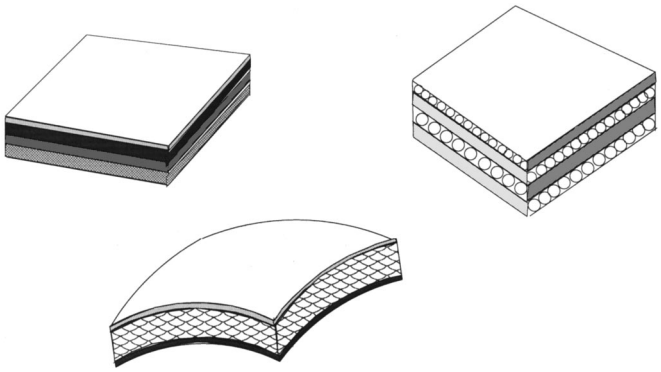

Fig. 1 Examples of multilayer structures: Plates (upper part) made of layers of different materials (left) and by unidirectional fibers (right) and sandwich shell (lower part)

As a direct consequence of both TA and HTD, classical theories that were originally developed for traditional isotropic single-layer structures could be inadequate for prediction of the response of multilayered structures. Higher transverse deformability, in fact, demands the inclusion of transverse shear and normal stresses which are discarded in classical analyses. Furthermore, transverse discontinuous mechanical properties cause displacement fields $\boldsymbol{u} = (u_1, u_2, u_3)$ (bold letters denote arrays, while subscripts 1-2-3 denote the components in the 1-2-3 directions, respectively) in the thickness direction which can exhibit a rapid change of their slopes in correspondence to each layer interface (see Fig. 3). This is known as the *zig-zag (ZZ)* form of displacement fields in the thickness direction. In-plane stresses $\boldsymbol{\sigma}_p = (\sigma_{11}, \sigma_{22}, \sigma_{12})$ can, in general, be discontinuous at each layer interface (see Fig. 2). Nevertheless, transverse stresses $\boldsymbol{\sigma}_n = (\sigma_{13}, \sigma_{23}, \sigma_{33})$, for equilibrium reasons, ie, the Cauchy theorem, must be continuous at each layer interface (see Figs. 3 and 4). This is often referred to in the literature as *interlaminar continuity (IC)* of transverse stresses. Compatibility and equilibrium, ie, ZZ and IC, are strongly connected to each other. Figure 3 shows, from a qualitative point of view, how the scenarios of displacement $\boldsymbol{u}$ and transverse stress $\boldsymbol{\sigma}_n$ distributions in a multilayered structure could ap-

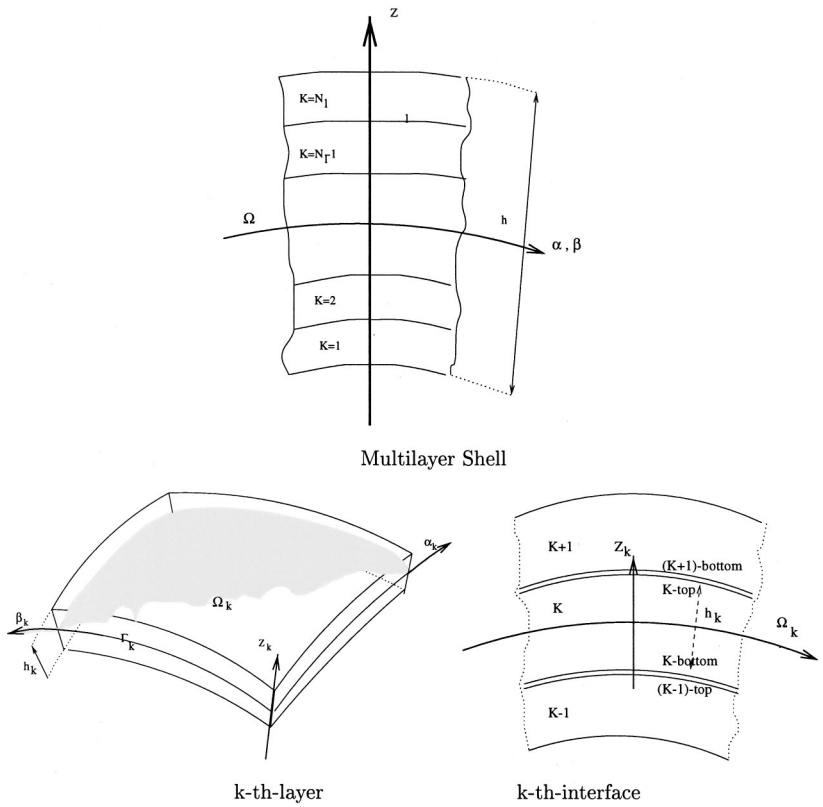

Fig. 2 Geometry and notations used for multilayered shells

pear in the exact solution and/or experiments. Stresses at the interfaces are displayed in Fig. 4. In-plane components, which can be discontinuous, are also depicted for comparison purpose. Figures 3 and 4 show that both displacement and transverse stresses, due to compatibility and equilibrium reasons, respectively, are C^0-continuous functions in the thickness z direction. $\boldsymbol{u}$ and $\boldsymbol{\sigma}_n$ have, in the most general case, discontinuous first derivatives with correspondence to each interface where the mechanical properties change. In [7,8], ZZ and IC were referred to as C_z^0-Requirements. The fulfillment of C_z^0-Requirements is a crucial point of two dimensional modeling of multilayered structures. In this respect, as it is clear in the next sections, RMVT offers a way of developing multilayered theories addressing the C_z^0-Requirements *completely* and *a priori*.

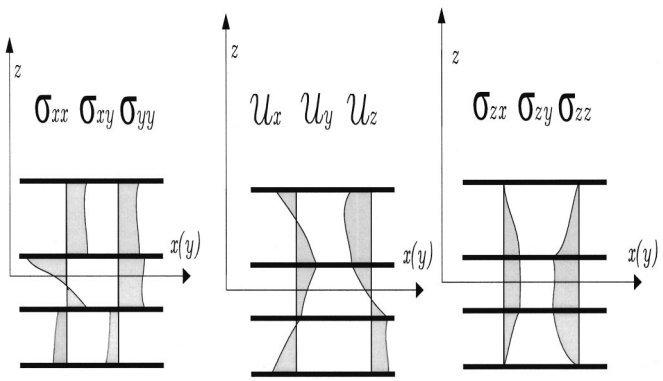

Fig. 3 Typical through the thickness stress (in-plane and transverse components) fields in a three layer plate: C_z^0-Requirements

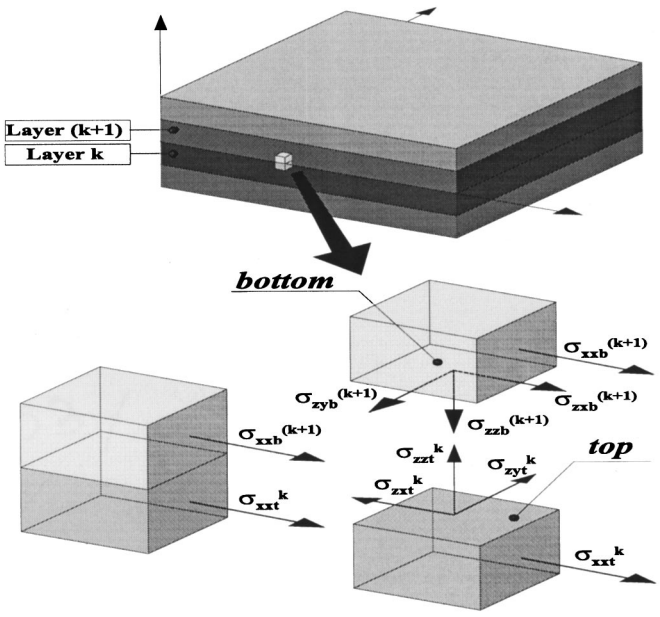

Fig. 4 Details and notations of stresses at the interface

2.2 Classical and refined approaches in view of the fulfillment of C_z^0-Requirements

Following Kraus [9], two-dimensional classical theories originally developed for single-layer structures made of traditional isotropic materials can be conveniently grouped as Love First Approximation Theories, LFAT or Love Second Approximation Theories, LSAT. The well known Cauchy-Poisson-Kirchhoff-Love [10–13] thin shell assumptions can be assigned to the first grouping: normals to the reference surface Ω remain normal in the deformed states and do not change in length. That is, transverse shear as well as normal strains are postulated to be negligible with respect to the other strains. Whenever LFAT postulates are totally or partially removed, the obtained theories are grouped into LSAT. It is of interest to emphasize that when developing LSAT, well known *Koiter's Recommendation* (KR) [9] should conveniently be taken into account. Such a recommendation, which was reached on the basis of energy considerations, states that:

> *a refinement of Love's first approximation theory is indeed meaningless, in general, unless the effects of transverse shear and normal stresses are taken into account at the same time*.

More general and systematic substantiation of Koiter's conclusion can be found in the books by Cicala [14,15] and Goldenveizer [16] in which the method of the asymptotic expansion of the three-dimensional governing equations has been employed.

A large amount of contributions in which LFAT and LSAT have been extended to multilayered structures have been presented in the literature. Applications of LFAT theories to multilayered structures are often referred to as the *Classical Lamination Theories* (CLT) (see Jones [17]). Extensions of the so-called Reissner [18] and/or Mindlin [19] LSAT type model, which includes transverse shear strains, to layered structures are known as the *Shear Deformation Theory* (SDT), (*or First order SDT, FSDT*) see Whitney [20] and the recent book by Reddy [21]. Koiter's recommendation can be fulfilled by including both transverse shear and normal strains as done by Hildebrand, Reissner, and Thomas [9]. Examples of applications of these types of models to laminated structures can be found in the works by Sun and Whitney [22], and Lo, Christensen, and Wu [23] which use LSAT similar to those proposed by Hildebrand, Reissner, and Thomas [4]. These all are known as *Higher Order Theories, (HOT)*. An excellent overview of these types of theories can be found in the book by Librescu [24].

The simple extension of LFAT or LSAT to multilayer structures does not permit the fulfillment of the C_z^0-Requirements; that is, ZZ and IC are not addressed by the CLT, SDT and HOT approaches mentioned above. An exception is given by Vlasov's [25] SDT-type theory which permits fulfillment of the homogeneous conditions (zero-values) for the transverse shear stresses in correspondence to the top and bottom shell/plate surfaces. Reddy [26] and Reddy and Phan [27] have shown that such a simple refinement of the SDT-type approach, could lead to significant improvement, with respect to the same SDT analyses, toward the prediction of the static and dynamic response of thick laminated structures.

The zig-zag effect is not accounted for in the previously discussed works. These all have a number of unknown variables that are independent of the number of the constitutive layers N_1. Following Reddy [21], these types of theories are here grouped as *Equivalent Single Layer Theories (ESLM)*. A possible natural manner of including the ZZ effect could be implemented by applying LFAT or LSAT at a layer level, that is, each layer is seen as an independent plate/shell and compatibility of displacement is then imposed as a constraint. In these cases *Layer Wise Models (LWM)* are obtained. Relevant examples of these types of theories are those found in the articles by Srinivas [28], who applied CLT in each layer, and by Cho, Bert, and Striz [29], who implemented the HOT by Lo, Christensen, and Wu [23] in each layer. Generalizations on these types of theories were given by Reddy and his coauthors [30,31] who expressed the displacement variables in the thickness direction in terms of Lagrange polynomials (interface values were used as unknown variables) therefore permitting an easy linkage of compatibility conditions at each interface.

The literature has shown that LWM provides much better results than do ESLM type analyses. However, the previously overviewed ESL or LW classical models, being formulated with only displacement unknowns, cannot *a priori* describe interlaminar equilibrium IC for the transverse stresses, ie, C_z^0-Requirements are not completely fulfilled. Applications of these theories in fact require *a posteriori* the recovery of transverse stresses. In this respect, it has been shown (see, [32,17]) that better results can be obtained by integrating the three-dimensional 3D equilibrium equations than the use of material constitutive equations (Hooke's law). On the other hand, the *a priori* fulfillment of transverse stress equilibria could introduce improvement for both in-plane and out-of-plane results.

Apart from the previously discussed contributions, special merit mention should be made of those works in which the description of both IC and ZZ effects is addressed. The first and most relevant contributions appeared in the Russian literature. Among these one should mention the pioneering paper by Lekhnitskii [33], the books by the same author [34], and by Ambartsumian [35] as well as the already mentioned article by Vlasov [25] and the recent overview paper by Grigolyuk and Kulikov [36]. Lekhnitskii's very elegant approach that was originally developed for beams, and which describes interlaminar continuous transverse shear stress as well as ZZ effects, was extended to plates by Ren [37]; Ambartsumian's theory, which describes both IC and ZZ effects, was first extended to unsymmetric cases by Whitney [20] and then to shell geometries by Rath and Das [38]. Hundreds of papers have been published based on these latter theories (see the overview papers mentioned at the end of Section 2.3). Most of the works based on these types of theories do not account for interlaminar continuous transverse normal stress σ_{33} description, ie, Koiter's recommendation is not

included. A recent example of an extension of Ambartsumian type-theory, directed to include σ_{33} effects, is the work by Aitharaju and Averill [39].

2.3 C_z^0-Requirements and RMVT

All the previously discussed theories are formulated on the basis of displacement variables. These types of theories are not designed to *a priori* provide interlaminar continuous transverse stresses. A post-processing procedure is required to recover $\boldsymbol{\sigma}_n$ stresses. Post-processing can be avoided only if stress assumptions are made. Both in-plane and transverse stresses can be assumed in the framework of mixed variational principles (see [40,41]). In such a context, as stated in the introduction, *Reissner's Mixed Variational Theorem consists of a mixed principle designed for multilayered structures*. RMVT, in fact, restricts the stress assumptions to transverse components. Murakami [42–44] was the first to apply RMVT to multilayered structures by assuming two independent fields for displacement and transverse stresses variables. Toledano and Murakami [45,46] showed that RMVT does not experience any particular difficulties when including transverse normal stresses in a plate theory. The ways in which RMVT can be applied, a discussion on the various contributions documented in literature, and the related results are dealt with in the following sections.

To be complete it must be underlined that only a few contributions on two dimensional modeling of multilayered plates and shells have been discussed. It is not the aim of this article to mention all of them. A complete discussion on the several contributions that appeared in the literature has been covered by recent exhaustive state-of-the-art articles. Among these one can mention the papers by Librescu and Reddy [47]; Kapania [48]; Kapania and Raciti [49]; Noor and Burton [50,51]; Reddy and Robbins [52]; Soldatos and Timarci [53]; Noor, Burton, and Bert [54]; and the books by Librescu [24] and Reddy [21].

3 REISSNER MIXED VARIATIONAL THEOREM (RMVT)

For a complete and rigorous understanding of the foundations of RMVT, reference can be made to the articles by Professor Reissner [1–3]. Readers can refer to these works for a systematic comprehension of the mathematical/variational background of Reissner's Theorem. Here the author's aim is to try to give a simple interpretation of RMVT, starting from the basic concept of continuum mechanics and the well known statements of calculus of variations (see, [40,41,55]).

In solid mechanics, it is well known that the Principle of Virtual Displacement (PVD) involves only a compatible displacement field as a variable and has for its Euler-Lagrange equations the conditions of balance of momenta and traction boundary conditions. Likewise, the dual form of PVD, ie, the Principle of Virtual Forces (PVF), involves a stress field which is equilibrated and satisfies the traction boundary conditions, alone as a variable and has the kinematic compatibility conditions and displacement boundary conditions as its Euler-Lagrange equations. If in PVD kinematic compatibility and displacement boundary conditions are introduced as conditions of constraint through Lagrange multipliers, which turn out to be stresses and surface traction respectively, one then obtains the so-called Hu-Washizu Variational Principle. Likewise, if the conditions of equilibrium of stresses are introduced as a constraint condition through a Lagrange multipliers field (which turns out to be displacement) into PVF, one is led to the so-called Hellinger-Reissner principles. Thus, the Hu-Washizu and Hellinger-Reissner principles, which involve that one field in the continuum as variables (some of which play the role of Lagrange multipliers to enforce certain constraint conditions), are often referred to as mixed variational principles.

This is the scenario in which RMVT can be simply interpreted as a particular case of the previously mentioned mixed principles in which *only* compatibility of transverse strain $\boldsymbol{\epsilon}_n=(\epsilon_{13},\epsilon_{23},\epsilon_{33})$ is enforced by means of Lagrange multipliers which, in this case, turn out to be transverse stresses $\delta\boldsymbol{\sigma}_n=(\delta\sigma_{13},\delta\sigma_{23},\delta\sigma_{33})$ (δ is the variational symbol). As mentioned in the introduction, the word *only* signifies Reissner's intuition: for multilayered structure analyses it is sufficient to restrict the mixed assumptions to transverse stresses. It is for such stresses that an independent field is in fact required to *a priori* and *completely* fulfill the C_z^0-Requirements. The remaining part of this subsection quotes the equations related to PVD and RMVT, according to the notations that are used in this paper.

PVD assumes a displacement field $\boldsymbol{u}$ and puts 3D indefinite equilibrium (and related equilibrium conditions at the boundary surfaces which are, for the sake of brevity, not written here) into a variational form. In the dynamic case, these equations are

$$\sigma_{ij_{,i}}-\rho\ddot{u}_i=p_i \quad i,j=1,2,3 \tag{1}$$

where ρ is the mass density and double dots denote accelerations while $p=(p_1,p_2,p_3)$ are body forces. The corresponding PVD integral, variational equation for a multilayered structure is written as:

$$\int_V(\delta\boldsymbol{\epsilon}_{pG}^T\boldsymbol{\sigma}_{pH}+\delta\boldsymbol{\epsilon}_{nG}^T\boldsymbol{\sigma}_{nH})dV=\int_V\rho\,\delta\mathbf{u}\ddot{\mathbf{u}}dV+\delta L_e \tag{2}$$

The superscript T signifies an array transposition and V denotes the 3D multilayered body volume while the subscripts n and p denote transverse (out-of-plane, normal) and in-plane components, respectively. Therefore $\boldsymbol{\sigma}_p=\{\sigma_{11},\sigma_{22},\sigma_{12}\}$, $\boldsymbol{\sigma}_n=\{\sigma_{13},\sigma_{23},\sigma_{33}\}$ and $\boldsymbol{\epsilon}_p=\{\epsilon_{11},\epsilon_{22},\epsilon_{12}\}$, $\boldsymbol{\epsilon}_n=\{\epsilon_{13},\epsilon_{23},\epsilon_{33}\}$. The subscript H underlines that stresses are computed via Hooke's law. The variation of the internal work has been split into in-plane and out-of-plane parts and involves stress from Hooke's law and strain from geometrical relations (subscript G). δL_e is the virtual variation of the work made by the external layer-force **p**.

RMVT can be simply constructed by adding the constraint equations for the transverse stresses to PVD. These equations can be built by evaluating transverse strains in two manners: by Hooke's law $\boldsymbol{\epsilon}_{nH}$ and by a geometrical relations $\boldsymbol{\epsilon}_{nG}$. In formula

$$\boldsymbol{\epsilon}_{nH} - \boldsymbol{\epsilon}_{nG} = 0 \tag{3}$$

RMVT therefore states

$$\int_V (\delta \boldsymbol{\epsilon}_{pG}^T \boldsymbol{\sigma}_{pH} + \delta \boldsymbol{\epsilon}_{nG}^T \boldsymbol{\sigma}_{nM} + \delta \boldsymbol{\sigma}_{nM}^T (\boldsymbol{\epsilon}_{nG} - \boldsymbol{\epsilon}_{nH})) dV$$

$$= \int_V \rho \, \delta \mathbf{u} \ddot{\mathbf{u}} dV + \delta L_e \tag{4}$$

The third 'mixed' term variationally enforces the compatibility of the transverse strain components. Subscript *M* underlines that transverse stresses are those of assumed model.

4 USE OF RMVT TO DEVELOP PLATE/SHELL THEORIES

This section shows how RMVT can be used as a tool to develop two-dimensional modelings of multilayered structures. These developments are presented in the most general cases of *N*-order for the expansion of the unknown variable in the *z*-thickness coordinate.

In the so-called axiomatic approach framework, certain displacement and/or stress fields are postulated in the plate *z*-direction. An interesting discussion on the implications of the axiomatic character of a given theory has been provided by Antona [56]. According to the variational statements, two-dimensional theories for flat and curved structures could be formulated according to the following four steps.

1) Displacement and/or stress distributions in the thickness plate/shell direction *z*, are *postulated* by referring to a certain set of base functions.
2) Material behavior is assigned, ie, Hooke's law is given.
3) A geometrical relation is given, ie, a strain-displacement relation is assumed.
4) Variational statements are then used to establish governing equations. These equations could be given in the following two manners:
   - 4.1) *strong form* (integration by part and boundary conditions are written as a system of differential equations that hold in each point of the plate/shell in-plane domain Ω).
   - 4.2) *weak form* (further to *z* assumption at point 1, additional approximations are introduced in the plate/shell domain Ω, and the resulting equations are written as a system of algebraic equations).

This section discusses the previous points in four different subsections. Two examples of applications of RMVT which provide strong and weak forms of governing equations are given in detail in Appendices A and B, respectively. The first Appendix deals with multilayered shells, while the second deals with Finite Element (FE) formulation of multilayered plates.

4.1 Displacement and transverse stress assumptions in a unified form

The behavior of a displacement and/or transverse stress component, here denoted by *f*, is postulated in the thickness plate *z*-directions according to a given expansion

$$f(x,y,z) = F_i(z) f_i(x,y) \quad i = 1, N^* \tag{5}$$

It is intended that repeated indexes are summed over their ranges. The polynomials $F_i(z)$ constitute a set of independent functions. Such a base can be arbitrarily chosen: the power of *z* and combinations of Legendre polynomials are considered in this paper. N^* denotes the number of the introduced terms. In the case of classical models formulated on the basis of PVD, the assumptions of Eq. (5) are restricted to the displacement variables. Traditionally *z* power expansion is employed,

$$\mathbf{u} = \mathbf{u}_0 + z^r \mathbf{u}_r, \quad r = 1,2,..,N \tag{6}$$

Subscript 0 denotes displacement values in correspondence to the plate/shell reference surface Ω, which does not necessarily correspond to the middle plate/shell surface. Linear and higher order distributions are introduced in the *z*-direction by the *r*-polynomials. *N* remains a free parameter of the model. Different *N* values could be used for different displacement and stress components.

In order to write the complete modelings in a unified notation, the previous expansion is rewritten in the following manner,

$$\mathbf{u} = F_t \mathbf{u}_t + F_b \mathbf{u}_b + F_r \mathbf{u}_r = F_\tau \mathbf{u}_\tau, \quad \tau = t,b,r,$$
$$r = 1,2,..,N-1 \tag{7}$$

By comparing Eq. (7) to Eq. (6), one finds out that subscript *b* denotes values in correspondence to Ω ($\mathbf{u}_b = \mathbf{u}_0$) while subscript *t* refers to the highest order term ($\mathbf{u}_t = \mathbf{u}_N$). The F_τ polynomials assume the following explicit form:

$$F_b = 1, \quad F_t = z^N, \quad F_r = z^r, \quad \mathbf{r} = 1,2,..,N-1 \tag{8}$$

The *b* and *t* subscripts also signify (see below), values of the displacement and/or stress variables in correspondence to layer bottom and layer top surfaces, respectively.

The assumptions written for previous expansions can be made at the layer or the multilayered level. Layer-wise (LW) and Equivalent Single Layer (ESLM) descriptions correspond to former and latter cases, respectively. These are discussed separately in the following two subsections.

4.1.1 Equivalent single layer models (ESLM)

The displacement variables are the same in each of the N_l-layers. In such a framework, the expansion given in Eq. (6) does not permit the description of the zig-zag effects. Such a limitation could somehow be overcome by referring to Murakami's idea. Murakami [44] proposed adding a zig-zag function to Eq. (5),

$$\mathbf{u} = \mathbf{u}_0 + (-1)^k \zeta_k \mathbf{u}_Z + z^r \mathbf{u}_r, \quad r = 1,2,..,N \tag{9}$$

Subscript *Z* refers to the introduced zigzag term. Note that the unknown variables $\mathbf{u}_0, \mathbf{u}_Z, \mathbf{u}_r$ are *k*-independent. The geometrical meaning of the zig-zag function is explained in Fig. 5 (see also the EMZ1, EMZC3, EDZ1, EDZ3 cases depicted in Fig. 7). $\zeta_k = 2z_k/h_k$ is a non-dimensioned layer coordinate. z_k is the physical coordinate of the *k*-layer whose thickness is h_k. The exponent *k* changes the sign of the zig-zag term in each layer. Such an artifice permits one to reproduce

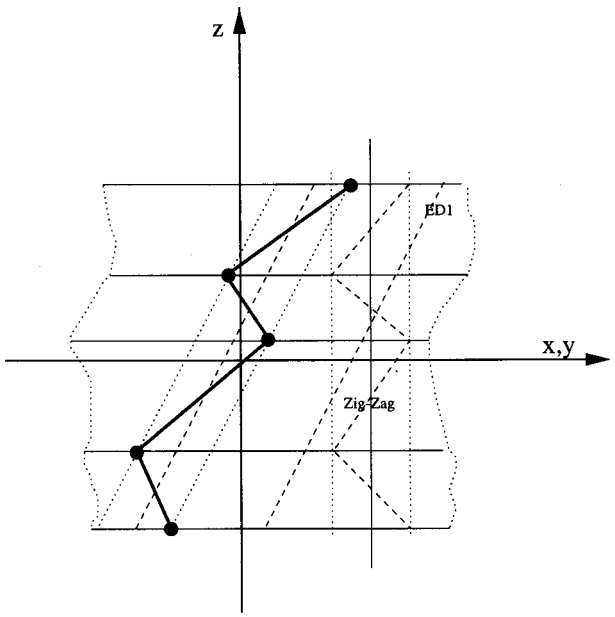

Fig. 5 Geometrical meaning of zig-zag function, Linear case

the discontinuity of the first derivative of the displacement variables in the z-directions which physically comes from the intrinsic transverse anisotropy TA of multilayer structures (as depicted in Fig. 3].

By employing a unified notation Eq. (9) becomes,

$$\boldsymbol{u}=F_t\boldsymbol{u}_t+F_b\boldsymbol{u}_b=F_r\boldsymbol{u}_r=F_\tau\boldsymbol{u}_\tau,\tau=t,b,r,\quad r=1,2,..,N \tag{10}$$

Subscript t has been chosen to denote the zig-zag term, ie $\boldsymbol{u}_t=\boldsymbol{u}_z$ and $F_t=(-1)^k\zeta_k$.

The Taylor type expansion of Eq. (6) is not convenient for the transverse stress assumptions. Transverse stress variables in fact demand a layer-wise description to be able to fulfill the C_z^0-requirements. A convenient combination of Legendre polynomials [7,44–46] could be used as a base functions,

$$\boldsymbol{\sigma}_{nM}^k=F_t\boldsymbol{\sigma}_{nt}^k+F_b\boldsymbol{\sigma}_{nb}^k+F_r\boldsymbol{\sigma}_{nr}^k=F_\tau\boldsymbol{\sigma}_{n\tau}^k,\quad \tau=t,b,r,$$
$$r=2,3,..,N;\quad k=1,2,..,N_1 \tag{11}$$

It is now intended that the subscripts t and b denote values related to the top- and bottom-layer surfaces, respectively. These two terms consist of the linear part of the expansion. The thickness functions $F_\tau(\zeta_k)$ have now been defined at the k-layer level,

$$F_t=\frac{P_0+P_1}{2},\quad F_b=\frac{P_0-P_1}{2},\quad F_r=P_r-P_{r-2},$$
$$r=2,3,..,N \tag{12}$$

in which $P_j=P_j(\zeta_k)$ is the Legendre polynomial of the j-order defined in the ζ_k-domain: $-1\leqslant\zeta_k\leqslant1$. For instance, the first five Legendre Polynomials are

$$P_0=1,\quad P_1=\zeta_k,\quad P_2=(3\zeta_k^2-1)/2,$$
$$P_3=\frac{5\zeta_k^3}{2}-\frac{3\zeta_k}{2},\quad P_4=\frac{35\zeta_k^4}{8}-\frac{15\zeta_k^2}{4}+\frac{3}{8}$$

The chosen functions have the following properties:

$$\zeta_k=\begin{cases}1:F_t=1; & F_b=0; & F_r=0\\ -1:F_t=0; & F_b=1; & F_r=0,\end{cases} \tag{13}$$

The top and bottom values have been used as unknown variables. Such a choice makes the model particularly suitable, in view of the fulfillment of the C_z^0-Requirements. The interlaminar transverse shear and normal stress continuity IC can therefore be linked by simply writing:

$$\boldsymbol{\sigma}_{nt}^k=\boldsymbol{\sigma}_{nb}^{(k+1)},\quad k=1,N_l-1 \tag{14}$$

In those cases in which the top/bottom plate/shell stress values are prescribed (zero or imposed values), the following additional static conditions must be accounted for:

$$\boldsymbol{\sigma}_{nb}^1=\overline{\boldsymbol{\sigma}}_{nb},\quad \boldsymbol{\sigma}_{nt}^{N_l}=\overline{\boldsymbol{\sigma}}_{nt} \tag{15}$$

where the over-bar denotes the prescribed values in correspondence to the plate/shell boundary surfaces. This makes it evident that the *a priori* and *complete* fulfillment of the C_z^0-Requirements demands a LW description for transverse stresses. In this sense, ESLM implicitly signifies that ESLM assumptions are restricted to the displacement variables. A full ESLM description could be acquired by expressing the stress variables in terms of the displacement variables. A way of doing this is described in Section 5 where the so-called *Weak Form of Hooke's Law* is presented.

4.1.2 Layer-wise model (LWM)

A full layer-wise description can be introduced by simply extending the stress assumptions of the previous paragraph to displacement variables,

$$\boldsymbol{u}^k=F_t\boldsymbol{u}_t^k+F_b\boldsymbol{u}_b^k+F_r\boldsymbol{u}_r^k=F_\tau\boldsymbol{u}_\tau^k \qquad \tau=t,b,r$$
$$r=2,3,..,N$$
$$\boldsymbol{\sigma}_{nM}^k=F_t\boldsymbol{\sigma}_{nt}^k+F_b\boldsymbol{\sigma}_{nb}^k+F_r\boldsymbol{\sigma}_{nr}^k=F_\tau\boldsymbol{\sigma}_{n\tau}^k \quad k=1,2,..,N_l \tag{16}$$

In addition to Eq. (14), the compatibility of the displacement reads

$$\boldsymbol{u}_t^k=\boldsymbol{u}_b^{(k+1)},\quad k=1,N_l-1 \tag{17}$$

It should be noticed that LW description does not require any zig-zag function for the simulation of the zig-zag effects. C_z^0-Requirements are completely and *a priori* fulfilled by Eqs. (14)–(17).

4.1.3 Summary of possible plate/shell theories

Depending on the variational statement used (PVD or RMVT), the description of the variables (LWM or ESLM), the order of the expansion used N, a number of two-dimensional theories can be constructed. In order to express different theories in a concise manner, acronyms could conveniently be used. These acronyms have here been formed as illustrated in Fig. 6. Extensive use of such acronyms will be made in the numerical overview reported in Section 7. Examples of displacement and stress fields related to particular-case theories have been plotted in Fig. 7. A few comments on these plots follow. Transverse stress and displacement z-fields have z-distribution for mixed cases: LM1 (Layer-

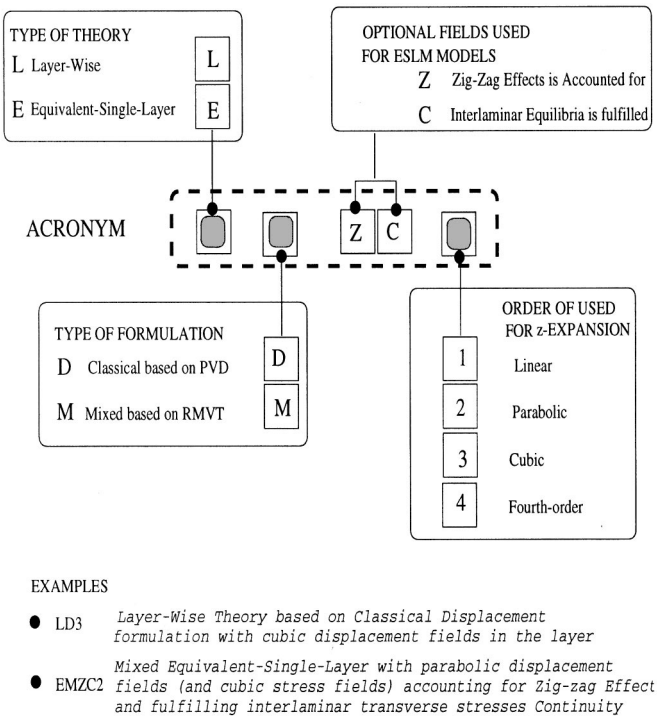

Fig. 6 Meanings of the used acronyms

wise Mixed, linear) and LM3 (Layer-wise Mixed, cubic). Only displacement assumptions are made for LD1 (Layer-wise Displacement, linear) and LD3 (Layer-wise Displacement, cubic) cases. A parabolic transverse stress field in each-layer is associated with a linear zig-zag displacement field for the EMZC1 case (Equivalent-single-layer Mixed including Zig-zag and interlaminar-Continuity, linear) and fourth-order transverse stress field in each-layer is associated with a cubic zig-zag displacement field for the EMZC3 case (Equivalent-single-layer Mixed including Zig-zag and interlaminar-Continuity, cubic). Note the geometrical meaning of the use of the zig-zag function: a linear through the thickness function of constant amplitude and the opposite sign for two adjacent layers has been added to a Taylor-type, linear (or cubic for EMZC3) ESL *z*-distribution to force discontinuous derivatives at each interface for the displacement components.

4.2 Hooke's law

The laminae are considered to be homogeneous and to operate in the linear elastic range. By employing stiffness coefficients, Hooke's law for the anisotropic *k*-lamina is written in the form $\sigma_i = \widetilde{C}_{ij}\epsilon_j$, where the sub-indices *i* and *j*, ranging from 1 to 6, stand for the index couples 11, 22, 33, 13, 23, and 12, respectively. The material is assumed to be orthotropic, as specified, by: $\widetilde{C}_{14}=\widetilde{C}_{24}=\widetilde{C}_{34}=\widetilde{C}_{64}=\widetilde{C}_{15}=\widetilde{C}_{25}=\widetilde{C}_{35}=\widetilde{C}_{65}=0$. This implies that σ^k_{13} and σ^k_{23} depend only on ϵ^k_{13} and ϵ^k_{23}. In matrix form,

$$\boldsymbol{\sigma}^k_{pH} = \widetilde{\mathbf{C}}^k_{pp}\boldsymbol{\epsilon}^k_{pG} + \widetilde{\mathbf{C}}^k_{pn}\boldsymbol{\epsilon}^k_{nG}$$
$$\boldsymbol{\sigma}^k_{nH} = \widetilde{\mathbf{C}}^k_{np}\boldsymbol{\epsilon}^k_{pG} + \widetilde{\mathbf{C}}^k_{nn}\boldsymbol{\epsilon}^k_{nG} \qquad (18)$$

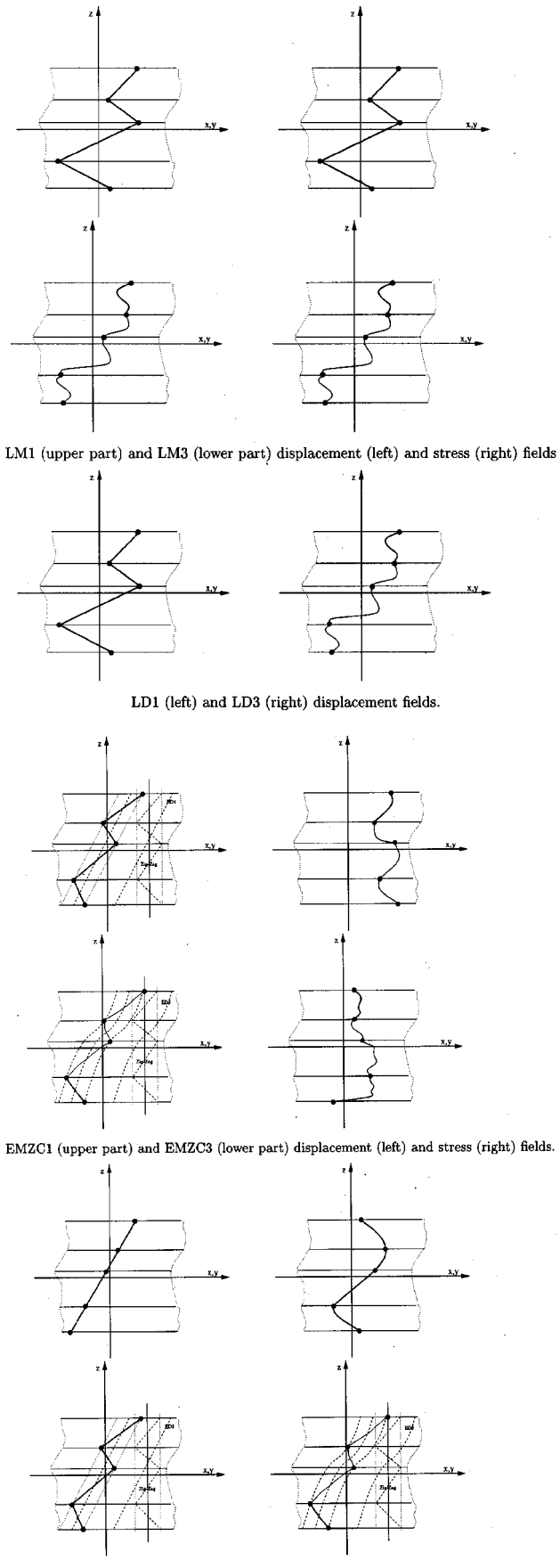

LM1 (upper part) and LM3 (lower part) displacement (left) and stress (right) fields

LD1 (left) and LD3 (right) displacement fields.

EMZC1 (upper part) and EMZC3 (lower part) displacement (left) and stress (right) fields.

ED1, ED3 (upper part) and EDZ1 and EDZ3 (lower part) displacement fields.

Fig. 7 Examples of assumed fields in the thickness plate direction in a four layer plate

In explicit form the matrices are,

$$\tilde{\mathbf{C}}^k_{pp}=\begin{bmatrix}\tilde{C}^k_{11} & \tilde{C}^k_{12} & \tilde{C}^k_{16}\\ \tilde{C}^k_{12} & \tilde{C}^k_{22} & \tilde{C}^k_{26}\\ \tilde{C}^k_{16} & \tilde{C}^k_{26} & \tilde{C}^k_{66}\end{bmatrix},\quad \tilde{\mathbf{C}}^k_{pn}=\tilde{\mathbf{C}}^{k^T}_{np}=\begin{bmatrix}0 & 0 & \tilde{C}^k_{13}\\ 0 & 0 & \tilde{C}^k_{23}\\ 0 & 0 & \tilde{C}^k_{36}\end{bmatrix},$$

$$\tilde{\mathbf{C}}^k_{nn}=\begin{bmatrix}\tilde{C}^k_{44} & \tilde{C}^k_{45} & 0\\ \tilde{C}^k_{45} & \tilde{C}^k_{55} & 0\\ 0 & 0 & \tilde{C}^k_{66}\end{bmatrix}.$$

It should be noticed that σ_{33} couples the in-plane and out-of-plane stress and strain components. The application of RMVT Eq. (4) requires transverse strains from Hooke's law. The stress-strain relationships are therefore put in the following mixed form (see also [24])

$$\boldsymbol{\sigma}^k_{pH}=\mathbf{C}^k_{pp}\boldsymbol{\epsilon}^k_{pG}+\mathbf{C}^k_{pn}\boldsymbol{\sigma}^k_{nM}$$
$$\boldsymbol{\epsilon}^k_{nH}=\mathbf{C}^k_{np}\boldsymbol{\epsilon}^k_{pG}+\mathbf{C}^k_{nn}\boldsymbol{\sigma}^k_{nM} \tag{19}$$

where both stiffness and compliance coefficients are employed. The subscript *M* states that the transverse stresses are those of the assumed model. The relation between the arrays of coefficients in the two forms of Hooke's law is simply found

$$\mathbf{C}^k_{pp}=\tilde{\mathbf{C}}^k_{pp}-\tilde{\mathbf{C}}^k_{pn}\tilde{\mathbf{C}}^{k^{-1}}_{nn}\tilde{\mathbf{C}}^k_{np},$$
$$\mathbf{C}^k_{pn}=\tilde{\mathbf{C}}^k_{pn}\tilde{\mathbf{C}}^{k^{-1}}_{nn}\quad \mathbf{C}^k_{np}=-\tilde{\mathbf{C}}^{k^{-1}}_{nn}\tilde{\mathbf{C}}^k_{np},\quad \mathbf{C}^k_{nn}=\tilde{\mathbf{C}}^{k^{-1}}_{nn}$$

Superscript -1 denotes an inversion of the array.

4.3 Geometrical relation

Within the small deformation theory, the strain components $\boldsymbol{\epsilon}_p, \boldsymbol{\epsilon}_n$ are linearly related to the displacements $\boldsymbol{u}$ according to the differential, geometrical relations. These can be formally written as:

$$\boldsymbol{\epsilon}_{pG}=\mathbf{D}_p\boldsymbol{u},\quad \boldsymbol{\epsilon}^k_{nG}=\mathbf{D}_n\boldsymbol{u} \tag{20}$$

The explicit form of differential arrays $\mathbf{D}_p$ and $\mathbf{D}_n$, for the two cases of Cartesian and curvilinear coordinate systems, are given in Appendices A and B, respectively.

4.4 Governing equations

Only guidelines are given in this Section. More details related to two particular cases are given in the two Appendices.

4.4.1 Strong form

As usual in the application of variational calculus (Washizu [55], Reddy [40]), a strong form of governing equations requires the application of integration by parts and of Green's Theorem. Such a need permits one to convert the derivative with respect to the coordinates on Ω (middle surface) from the virtual variation of variables to the variables themselves. As a result, the governing equations are obtained in a differential form, on both domain Ω and their boundary Γ (Γ_g, Γ_m denotes those parts of Γ on which the geometrical and mechanical boundary conditions are prescribed, respectively). Upon substitution of the given displacement and the transverse stress models described in Section 4.1, as well as a given Hooke's law (Section 4.2), and strain displacement relations (Section 4.3), in conjunction with integration by part formulas, RMVT leads to a differential system of governing equations and related boundary conditions for each *k*-layer. The first set can be formally expressed in the following form

$$\delta\boldsymbol{u}^k_\tau:\quad \mathbf{K}^{k\tau s}_{uu}\boldsymbol{u}^k_{\mathbf{s}}+\mathbf{K}^{k\tau\mathbf{s}}_{u\sigma}\boldsymbol{\sigma}^k_{n\mathbf{s}}=\mathbf{M}^{k\tau s}\ddot{\boldsymbol{u}}^k_s+\mathbf{p}^k_\tau$$
$$\delta\boldsymbol{\sigma}^k_{n\tau}:\quad \mathbf{K}^{k\tau s}_{\sigma u}u^k_s+\mathbf{K}^{k\tau s}_{\sigma\sigma}\sigma^k_{n\mathbf{s}}=0 \tag{21}$$

The first line of equations, being related to $\delta\boldsymbol{u}^k_\tau$ variations, represents equilibrium conditions. The second line of equations, being related to $\delta\boldsymbol{\sigma}^k_{n_\tau}$ variations, represents compatibility equations. The further subscript *s* has been introduced to distinguish *z*-expansions for the variations of unknown variables from those used in the finite form of the same variables. Each term of the introduced arrays $\mathbf{K}^{k\tau s}_{uu}, \mathbf{K}^{k\tau s}_{u\sigma}, \mathbf{M}^{k\tau s}, \mathbf{K}^{k\tau s}_{\sigma u}, \mathbf{K}^{k\tau s}_{\sigma\sigma}$ is a product of differential operators, stiffness/compliance or inertia coefficients, and geometrical parameters.

The application of Green's Theorem produces boundary conditions that should be associated with the above written equilibrium equations. This second set of governing equations at the boundary can be formally written as follows,

$$\textit{geometrical on } \Gamma^g_k \quad \textit{mechanical on } \Gamma^m_k$$
$$\boldsymbol{u}^k_\tau=\bar{\boldsymbol{u}}^k_\tau \quad \text{or} \quad \mathbf{\Pi}^{k\tau s}_u\boldsymbol{u}^k_s+\mathbf{\Pi}^{k\tau s}_\sigma\boldsymbol{\sigma}^k_{ns}=\mathbf{\Pi}^{krs}_u\bar{\boldsymbol{u}}^k_s+\mathbf{\Pi}^{k\tau s}_\sigma\bar{\boldsymbol{\sigma}}^k_{ns} \tag{22}$$

in which the bar denotes assigned values. The arrays in the boundary terms possess the same structures as those in the equilibrium and constitutive equations.

By varying subscripts τ and *s* over their ranges, the explicit forms of *k*-layer governing equations are obtained. By varying *k* over its range, the corresponding equations of the N_l layer are obtained. The C^0_z-Requirements (Eqs. (14), (15), and (17)) can be imposed at this stage. The use of top-bottom layer values is particularly effective at this stage. Eqs (14), (15), and (17) can in fact be easily introduced into both the variations ($\delta\boldsymbol{u}^k_\tau, \delta\boldsymbol{\sigma}^k_{n\tau}$) and finite values ($\boldsymbol{u}^k_s, \boldsymbol{\sigma}^k_{n_s}$) of the unknown variables. Such operations naturally lead to governing equations at multilayer level.

4.4.2 Weak form

The closed form solutions of the equations written in the previous paragraph are only possible in very few cases, mainly those related to simple geometry, particular boundary conditions, laminated lay-outs, and linear problems. In most general cases, an approximate procedure is required to provide approximate solutions. In such a context, to write a weak form of governing equations becomes a necessity. Equilibrium and compatibility conditions related to RMVT are only fulfilled in the integral sense: these appear as a system of algebraic equations.

Among the possible approximate methods (see, [7]) here attention is focused on the Finite Element Method (FEM). According to this method, displacement and stress variables are further expressed in terms of their values at the nodes of a given element (see for example, [7,57]),

$$\boldsymbol{u}_{\tau}^{k}=R_i\mathbf{q}_{\tau i}^{k}\quad (i=1,2,\ldots,N_n) \tag{23}$$

$$\boldsymbol{\sigma}_{n\tau}^{k}=R_i\mathbf{g}_{\tau i}^{k}\quad (i=1,2,\ldots,N_n) \tag{24}$$

in which N_n is the number of nodes of the element and R_i is the shape function related to the *i*-node. Upon substitution of the displacement model, Hooke's law, and finite element approximations, (integration by parts is now not required, the derivatives on the virtual variation are in fact moved to the nodal values which are unknown nodal values, not unknown functions), RMVT leads to a weak form of governing equations. These are formally written as in the strong form case,

$$\begin{aligned}\delta\mathbf{q}_{\tau i}^{kT}:\quad & \mathbf{K}_{uu}^{k\tau sij}\mathbf{q}_{sj}^{k}+\mathbf{K}_{u\sigma}^{k\tau sij}\mathbf{g}_{sj}^{k}=\boldsymbol{P}_{\tau i}^{k}\\ \delta\mathbf{g}_{\tau i}^{kT}:\quad & \mathbf{K}_{\sigma u}^{k\tau sij}\mathbf{q}_{sj}^{k}+\mathbf{K}_{\sigma\sigma}^{k\tau sij}\mathbf{g}_{sj}^{k}=0\end{aligned} \tag{25}$$

Each term of the introduced arrays $\mathbf{K}_{uu}^{k\tau s},\mathbf{K}_{u\sigma}^{k\tau s},\mathbf{M}^{k\tau s}\mathbf{K}_{\sigma u}^{k\tau s},\mathbf{K}_{\sigma\sigma}^{k\tau s}$ is now a number. These numbers are obtained by multiplying the stiffness/compliance or inertia coefficients, geometrical parameters, and the integrals of combinations of shape functions.

As far as the equations at the multilayered level are concerned, the C_z^0-Requirements must be used, as in the previous paragraph, to drive the governing equations from layers to a multilayer level, while assembly from the element to the structure level is made as usual as in the finite element technique.

An application with details on the formulation of a multilayered plate element is presented in Appendix B.

4.4.3 Treatment of stress variables

The coupled system of governing equations Eqs. (21), (22), and (25) can be solved in different ways. In the first, obvious case, stress and displacement variables are both retained and calculated at the same time, at the final stage of the implemented solution procedure. The second case is related to the possibilities of eliminating the stress variables (via constitutive equations) by expressing them in terms of the displacement unknowns. As an example, a static condensation-type procedure can be applied to Eq. (21). Stress variables are expressed by means of constitutive equations,

$$\delta\boldsymbol{\sigma}_{n\tau}^{k}:\boldsymbol{\sigma}_{ns}^{k}=(\mathbf{K}_{\sigma\sigma}^{k\tau s})^{-1}\mathbf{K}_{\sigma u}^{k\tau s}\boldsymbol{u}_{s}^{k} \tag{26}$$

The resulting equations, with only displacement variables, are

$$\delta\boldsymbol{u}_{\tau}^{k}:(\mathbf{K}_{uu}^{k\tau s}-\mathbf{K}_{u\sigma}^{k\tau s}(\mathbf{K}_{\sigma\sigma}^{k\tau s})^{-1}\mathbf{K}_{\sigma u}^{k\tau s})\boldsymbol{u}_{s}^{k}=\mathbf{M}^{k\tau s}\ddot{\boldsymbol{u}}_{s}^{k}+\mathbf{p}_{\tau}^{k} \tag{27}$$

It should be pointed out that this static condensation does not lead to those equations that could be obtained from direct application of PVD in the framework of displacement formulations. The array

$$\mathbf{K}_{uu}^{k\tau s}-(\mathbf{K}_{\sigma\sigma}^{k\tau s})^{-1}\mathbf{K}_{\sigma u}^{k\tau s}\mathbf{K}_{u\sigma}^{k\tau s}$$

in fact appears to be very much different from that obtained with PVD applications (see, [58,59,60,61], where displacement and mixed formulations are compared).

The treatments of stress variables above described has been referred to the *k*-layer. In practice, this should be done at a multilayer level right after the imposition of the C_z^0-Requirements. For those problems which involve non-homogeneous, transverse stress conditions, loadings arrays are involved in Eqs. (26) and (27).

Examples of the elimination of stress variables in strong form can be found in the work by Rao and Meyer-Piening [62] and more recently by Messina [63].

In the case of finite element applications, a further choice can be made. As is usual in FEM hybrid-implementation (see, [41]), stress variables can in fact be eliminated at an element level. The use of this type of technique makes the fulfillment of the C_z^0-Requirements weaker than the case of full mixed implementations.

A further possibility of eliminating the stress variables, and which the author believes to be of a certain relevance, is related to the use of a weak form of Hooke's law. The next section is devoted to this form.

5 A WEAK FORM OF HOOKE'S LAW

Full use of Reissner's theorem requires solving a problem in terms of both displacement and stress variables. This can result in a considerable expense. In order to preserve the advantages of a classical displacement formulation this section presents a *Weak Form of Hooke's Law (WFHL)*, which permits one to eliminate transverse shear and normal stress unknowns by expressing them, in a weak sense, in terms of the displacement ones. The WFHL was proposed by the author [64] who was completely inspired by RMVT.

The truncated Legendre expansion for displacement and transverse stress variables can be put in the weighted residual form in the thickness direction:

$$\int_{A_k}F_s(\boldsymbol{\epsilon}_{nG}^{k}-\boldsymbol{\epsilon}_{nH}^{k})dz=0,\quad s=t,b,2--N \tag{28}$$

As for the RMVT, Eq. (28) imposes compatibility of transverse strains. The difference is that the integral is now introduced only in the *z*-direction.

Substitution of a given displacement and the transverse stress models (Eqs. (6)–(11)) described in Sec. 4.1, as well as a given Hooke's law (Eq. (19)), and strain displacement relations (Eq. (20)), yields:

$$\int_{A_k}\mathbf{F}_s(\mathbf{D}_n\boldsymbol{u}^{k}-\mathbf{C}_{np}^{k}\boldsymbol{\epsilon}_{pG}^{k}+\mathbf{C}_{nn}^{k}\boldsymbol{\sigma}_{nM}^{k})dz=0 \tag{29}$$

By integrating along *z*, the set of Eq. (28) leads to a relation between transverse stress and displacement variables that can be formally written in the following array form:

$$\mathbf{H}_{u}^{k}\boldsymbol{u}^{k}-\mathbf{H}_{\sigma}^{k}\boldsymbol{\sigma}^{k}=0 \tag{30}$$

where $\mathbf{H}_{\sigma}^{k}$ is a square symmetric nonsingular matrix, while $\mathbf{H}_{u}^{k}$ is rectangular, singular and non symmetric. Examples of these matrices were reported by Carrera [7,64]. Equation (30), in conjunction with the interface constraints in Eqs (14), (15), and (17), permits one to write the constitutive equations at a multilayer level. This can be done by implementing the same assembly technique used for the governing equations of the previous paragraph.

Equation (28) can be interpreted as an automatic and variationally consistent procedure to compute correction factors for the transverse stress distributions along the thickness coordinates (it has an analogous meaning to the shear correction factors used in classical shear deformation theories).

WFHL remains very useful in FEM implementations. In particular it permits the extension of the C_z^0-Requirements (which are, in this context only, fulfilled in the weak sense) to existent displacement formulated finite elements. Numerical comparisons between full mixed implementation and the use of WFHL are unfortunately not yet available. These could be the subject of future work.

6 REVIEW OF AVAILABLE WORKS BASED UPON RMVT

This section has the main goal of reviewing those papers that apply RMVT to modeling of layered structures. Other types of applications are briefly mentioned in the last paragraph.

6.1 Beams

The effect of the coupling of stretching, bending, and transverse shearing deformation on the deflection of an anisotropic cantilever beam with a narrow rectangular cross-section has been investigated by Murakami and Yamakawa [65] and Murakami, Reissner, and Yamakawa [66]. Hierarchical beam models were developed upon application of RMVT. A particular case of WFHL, introduced by Carrera [7], was used by Aitharaju and Averill [39]. These authors restricted the WHFL in Eq. (28) to the transverse normal strains. Improvements in the evaluation of transverse normal strain energy were obtained for a layered beam, along with consistent results for normal strains and average transverse normal stress. As a further result, it was possible to eliminate Poisson's ratio locking in the associated finite-element model.

6.2 Plates

The first application of RMVT to modeling of multilayered flat structures was performed by Murakami [43,44], a scholar of Professor Reissner in San Diego. He introduced a first order ESL displacement field in his papers, in conjunction with an independent parabolic transverse stress LW field in each layer (transverse normal stress and strains were discarded). The ideas of zig-zag function as a tool to provide zig-zag effects in ESLM type theories was also introduced in the same papers. Cylindrical bending analyses of symmetric three and five-layer cross-ply simply supported plates were conducted. The comparison of the in-plane response to the exact solutions demonstrated that Murakami's theory led to accurate results even for small span-to-depth ratios. An extension to a higher order displacement field was proposed by Toledano and Murakami [45]. Parabolic and cubic terms were added to the Murakami's displacement field, while the transverse stress field became a fourth order one. Improvements were obtained compared to the Murakami's (1986) theory as far as asymmetric cross-ply laminates were concerned. Interlaminar continuous transverse stresses, including σ_{zz}, were considered in this last paper. Both linear [47] and higher order models [45] showed some limitations in the accurate descriptions of local stress for very thick plate cases. It became, in fact, clear to these two scientists that to keep constant the zig-zag function $\boldsymbol{u}_z$ of Eq. (9) in all layers, consists of a non-physical constraint. The effective behavior of laminated structures, as they appear from exact solutions, shows that the slope of the displacement field at layer interface is a layer property. That is, a full Layer-Wise description is required to accurately predict the behavior of a thick laminated plate. Toledano and Murakami in a subsequent paper [46] applied, in fact, RMVT in conjunction with a layer-wise description of both displacement and transverse stress fields. The displacement field was considered linear in each layer for the in-plane components u_x and u_y, while the transverse displacement was kept constant for the whole plate as in classical thin-plate assumptions. Transverse normal stress was discarded and transverse shear stresses were assumed to be parabolic in each layer. The numerical analysis showed that the accuracy of the obtained results was independent of the laminated configurations. Unfortunately, σ_{zz} and ϵ_{zz} effects were discarded by Toledano and Murakami [46]. Such a choice contrasts with Koiter's Recommendations, mentioned in Section 2.2. Note further that the simultaneous conditions $\sigma_{zz}=0$ and $\epsilon_{zz}=0$ are contradictory in nature. As a consequence, the obtained results showed limitations in the tracing of the response of very thick plates. Further discussions on RMVT were provided by Soldatos [67]. The three papers: Murakami [44], and Toledano and Murakami [45,46], should be considered as the fundamental works in the applications of RMVT as a tool to model multilayered structures.

A generalization, proposing a systematic use of RMVT as a tool to furnish a class of two dimensional theories for multilayered plate analysis, was presented by Carrera [7]. Even though this work was directed to the approximate solution technique, it reported most of the ideas that were used in subsequent works. The displacement and stress fields described in Eq. (16) were proposed in [7]. A further discussion was quoted in [8]. The order of displacement fields in the layer was taken as a free parameter of the theories. Applications of what is reported in [7,8] to derive governing equations in strong forms have been given in several other papers [61,68–75]. Closed-form solutions were also given in these papers and compared to exact solutions and to other available two-dimensional theories. Layer-wise mixed analyses were performed in Carrera [58] for the static case. Local and global responses were discussed and compared to three dimensional solutions and related classical analysis based on PVD. Linear and parabolic displacement and transverse stress fields were considered. As a fundamental result, the numerical analysis demonstrated that RMVT furnishes a quasi three-dimensional *a priori* description of transverse stresses, including transverse normal components. Sandwich plates were also considered in [69]. Governing equations for dynamic cases were given in (Carrera [58]). Related numerical analysis confirmed the suitability of RMVT to analyze static and dynamic responses of multilayered plates. Transverse normal stress effects in the static and dynamic case were discussed in [71,72]. In these works, RMVT showed that it is suitable to generate theories which can include or

discard transverse normal stresses, substantiating Koiter's Recommendations, as already mentioned in Section 2. These two works extended Koiter's Recommendations on multilayered structures in the following terms:

"*Any refinements of classical models are meaningless, unless the effects of interlaminar continuous transverse shear and normal stresses are both taken into account in a multilayered shell theory*."

Higher order displacement and stress fields (linear, up to fourth order) were considered in [71,72] and subsequent works. In [73], ESLM and LWM, based on RMVT, were compared. It was concluded that an LW description is required for very thick plate analysis. In particular, ESLM formulation experienced difficulties in describing transverse normal stresses and the related effects. It was further concluded that ESLM implementations, based on RMVT, have at least the same accuracy as other refined ESLM type theories based on different approaches. Different ways of computing transverse stresses were compared in [74]. Stresses from an assumed model, *a priori*, were compared to those calculated *a posteriori*, ie, from Hooke's law and by integration of three-dimensional indefinite equilibrium equations. ESLM and LWM were implemented in both RMVT and PVD cases. It was underlined that *a priori* transverse stresses can only be obtained by RMVT. It was mainly concluded that:

- *N*-order increasing, layer-wise analysis could furnish excellent *a priori* as well as *a posteriori* descriptions of transverse stresses of thick and thin laminated plates; ESLM accuracy remains subordinate to the laminate layout, to plate thickness and to two dimensional modelings (mixed results were much more accurate than classical ones).
- The discrepancy among the three manners of evaluating transverse shear stresses were barely dependent on the plate thickness ratio.

Recently, Messina [63] has compared RMVT results to PVD ones. Both cross-ply and angle-ply plates were analyzed. Transverse normal stresses were, however, discarded in this work.

RMVT has been also applied to trace the response of laminated plates subjected to thermal loadings which vary in the thickness direction. The superiority of RMVT formulated theories, compared to classical ones, was confirmed in [75]. The fundamental role of transverse normal strains for thermal loadings which vary in the thickness plate directions was underlined.

6.3 Shells

The first discussion on the application of RMVT to shells was also made by Reissner [3]. A particular case of the Toledano and Murakami [45,46,80] type theory was extended to cylindrical shells by Bhaskar and Varadan [76]. A cubic term was added to the in-plane displacement representation and the transverse shear stress field was taken to the fourth order in each layer. The good performance obtained by Toledano and Murakami was confirmed for shell geometries. It was further confirmed, by Bhaskar and Varadan, that applications of RMVT to the ESLM analyses do not directly yield accurate transverse shear stresses. Better results were in fact obtained by direct integration (*a posteriori*) of the equilibrium equations of three-dimensional elasticity compared to those given *a priori* by Eq. (11). Transverse normal stress was also discarded in the RMVT application proposed by Jing and Tzeng [77]. The same authors [78] claimed to be the promoters of a new mixed principle which was obtained by RMVT, by simply discarding the transverse normal stress σ_{zz} contributions. Discarding σ_{zz} obviously makes the derivation simpler than in the full RMVT applications: the in-plane and transverse stresses are in fact un-coupled in this case and consequently many terms disappear in the related governing equations. This particular case should, however, not be considered a new idea. It further contrasts with the well known, previously mentioned, Koiter's Recommendations. In the author's opinion, Jing and Tzeng's proposal further contrasts with Reissner's original aims. However, Jing and Tzeng, by extending Murakami's model [44] in conjunction with an accurate description of curvature terms, have shown the effectiveness of RMVT in analyzing moderately thick cylindrical shells.

A systematic extension of RMVT to shells has been proposed by Carrera in recent works [58–61,72]. Governing equations for doubly curved shells were derived for ESLM and LW cases in the static and dynamic cases. The good accuracy previously found for flat geometries was confirmed for curved panels and shells. Comparisons with three dimensional theories show the effectiveness of RMVT to give *a priori* a three-dimensional description of transverse stresses, including normal components. It was further shown that very thick shells demand an adequate description of curvature terms. Such a description was, in these terms, acquired by systematic use of fictitious interfaces in the layers.

6.4 Finite element models for plates and shells

The previously surveyed papers are mostly related to theoretical developments and present numerical evaluations in closed form. Closed form solutions can be given only for particular cases, mainly related to simply supported plates/shells of simple geometries (in-plane rectangular and constant curvatures) made by orthotropic materials and related to linear problems. More general and more practical problems require solutions in approximate form. In this context, finite element method plays a quite significant role.

A first FEM approach to multilayered structures, by means of RMVT, was presented by Jing and Liao [79]. A partial hybrid formulation was presented; a self equilibrated stress field was restricted to the three in-plane stresses. As usual in hybrid formulation, stress unknowns were eliminated at the element level in the implemented finite hexahedron element for each layer. The results were restricted to cross-ply plates and showed good accuracy as far as exact solutions and improvements were shown compared to other refined analyses.

Application of RMVT to develop standard finite elements was proposed by Rao and Meyer-Piening [62]. Toledano and Murakami's [80] theory was used. Stress unknowns were

Table 1. List of the Acronyms frequently used in tables and figures to denote results for multi-layered plates and shells, in alphabetic order

3D	Three Dimensional Solution
CLT	Classical Lamination Theory
C&P1, C&P3	HOT linear and cubic case after Cho and Parmerter [102]
D&P	HOT by Dennis and Palazotto [107]
D&S1, D&S3	HOT Linear and cubic case after Dischiuva [116]
EMZC1jt	EMZC theory by Jing and Tzeng [77,78]
EMZC1m	EMZC theory by Murakami [44]
EMZC3tm	EMZC3 theory by Toledano and Murakami [45,46,80]
EMZC3rm	EMZC3 finite element results by Rao and Meyer-Piening [62]
Exact	Exact, three-dimensional closed form solutions
FSDT	First order Shear Deformation Theory
HOT	Higher Order Theories
IK&T	HOT by Idlbi, Karama and Touratier [103]
K&K	HOT by Kant and Kommineni [117]
LC&W	HOT by Lo, Christensen and Wu [23]
PAR_{ds} , HYP_{ds} , UNI_{cs} , PAR_{cs} , HYP_{ds}	Several HOT considered by Timarci and Soldatos [109]
Ren	HOT by Ren [104]
ZZL	HOT by Dischiuva and Carrera [110]

eliminated before introducing FE approximations, by employing a technique which is equivalent to that referred here as WFHL (Section 5). That is, only displacements were taken as nodal variables in the ESLM framework. Applications were quoted for laminate and sandwich plates and were related to eight noded plate isoparametric elements. A generalization of RMVT as a tool to develop approximate solutions was given by Carrera [7]. Governing weak form equations and related matrix forms for the general cases of weighted residuals method applications were derived.

The extension of the standard Reissner-Mindlin model to multilayered structures was discussed by Carrera [64]. The finite plate elements obtained (four, eight and nine nodes) were denoted by the acronym RMZC, (Reissner Mindlin Zigzag Interlaminar Continuity). The obtained finite elements represent the FE implementation of the Murakami theory [44]. The weak form of Hooke's law proposed in [7] was used to eliminate transverse shear stress variables. The numerical efficiency of RMZC models in the nonlinear cases has been tested in subsequent works. Large deflection of postbuckling was analyzed by Carrera and Kröplin [81]. Nonlinear dynamic problems were solved by Carrera and Krause [82]. Applications to linear and nonlinear multilayered plates, embedding piezo layers, were given by Carrera [83]. Extensive applications to sandwich plates were quoted by Carrera and Niglia [84]. Corrected transverse shear stiffness was implemented by Carrera and Parisch [85] in large displacements; large rotations FE shell elements. Snap-back problems were also discussed in this paper. Partial and full extensions of RMZC to shell geometries have been done by Brank and Carrera [86,87] respectively. An assumed shear strain concept has been implemented by Brank and Carrera [87] to eliminate shear locking mechanisms and to prevent spurious modes which are typical of alternative reduced integration techniques.

All these applications have demonstrated that the RMZC finite element, formulated on the basis of RMVT, should be considered as the natural extension of well-known plate/shell elements, which are normally implemented in most commercial codes, to the analysis of multilayered structures. Systematic application of RMVT to developed ESLM, as well as LW multilayer plate elements, are in progress [88–90].

6.5 Other problems treated by employing RMVT

Few other applications of RMVT have been proposed in the specialized literature. These are here mentioned in a single, short section, because they are not the subject of the present paper.

As far as failure analysis of multilayered plates is concerned, the work by Toledano and Murakami [91] is of a certain interest. The problem of interlayer slip between two adjacent layers was modeled in [42,91,92] by employing RMVT. The theory was tested by examining cylindrical bending of two-layered plates. Murakami and co-authors [93–100] have also applied RMVT in the framework of mixture models. RMVT permitted one to synthesize fields with multi-variable field representations.

7 SELECTED RESULTS

A complete and exhaustive discussion, including details on the several applications of RMVT, can be found in the papers that have been surveyed in the previous section. The aim in this paper is to show through the help of significant examples, that:

- RMVT constitutes a valuable tool to analyze multilayer structures and that RMVT leads to a better description than classical analysis formulated with only displacement variables;
- RMVT can be applied to plate and shell geometries, to both linear and nonlinear problems as well as to closed form, analytical solutions and computational, FEM implementations;
- RMVT should be considered as the natural tool to analyze multilayer structures. In other words, RMVT plays the same role that PVD plays in the framework of single-layer, isotropic structures.

In order to identify all the modelings compared in this sec-

Table 2. Comparison of LM and LD type solutions to 3D Exact Solution by Noor and Burton [101] on stress and displacement fields. Simply-supported square bended by harmonic distribution of transverse pressure. Cross-ply skew-symmetric laminate with $N_l=10$, $G_{LT}/E_T = G_{Lz}/E_T = .50$, $G_{TT}/E_T = .35$, $\nu_{LT}=\nu_{Lz}=.30$, $\nu_{TT}=0.49$

a/h	E_L/E_T	z	3D	*Mixed*		*Classical*	
				LM2	LM1	LD2	LD1
			Transverse displacement $u_z \times \frac{E_T}{P^{N_l}_{z_t} h}$.				
	3	t	195.2	195.2	195.2	195.2	194.8
10		b	194.8	194.8	194.8	194.8	194.4
	30	t	52.31	52.31	52.27	52.31	52.13
		b	51.92	51.92	51.88	51.99	51.71
	3	t	14.59	14.59	14.59	14.59	14.55
5		b	14.17	14.17	14.17	14.17	14.13
	30	t	6.227	6.226	6.215	6.226	6.183
		b	5.838	5.838	5.827	5.838	5.794
			In-plane displacement $u_y \times \frac{E_T}{P^{N_l}_{s_t} h}$.				
10	3	t	−30.45	−30.45	−30.45	−30.45	−30.38
		b	27.40	27.40	27.40	27.40	27.33
	30	t	−7.017	−7.017	−7.011	−7.171	−6.985
		b	5.561	5.561	5.553	5.561	5.534
5	3	t	−3.784	−3.784	−3.784	−3.784	−3.769
		b	3.499	3.499	3.498	3.499	3.485
	30	t	−1.092	−1.092	−1.089	−1.092	−1.077
		b	0.767	0.767	0.763	0.767	0.754
			In-plane stress $\sigma_{yy} \times \frac{1}{P^{N_l}_{z_t}}$.				
10	3	t	13.02	13.02	13.02	13.02	13.71
		b	−29.62	−29.62	−29.62	−29.62	−30.17
	30	t	3.225	3.225	3.227	3.230	3.357
		b	−53.24	−53.24	−53.17	−53.24	−53.11
5	3	t	3.631	3.631	3.631	3.637	3.821
		b	−7.573	−7.576	−7.571	−7.578	−7.713
	30	t	1.326	1.326	1.323	1.331	1.372
		b	−14.71	−14.71	−14.63	−14.71	−14.51
			Transverse shear stress $\sigma_{yz} \times \frac{1}{P^{N_l}_{z_t}}$.				
10	3	c	2.380	2.380	2.370	2.380	2.375
	30	c	2.344	2.344	2.341	2.344	2.343
5	3	c	1.185	1.185	1.179	1.185	1.182
	30	c	1.141	1.141	1.383	1.141	1.142

tion, the unified notations of Section 4.1.3 are used. Other, additional theories are denoted by the acronyms listed in Table 1.

Closed-form solutions of Navier type governing equations, similar to those described in Appendix A, can be obtained by assuming harmonic distributions of the displacement and transverse stress variables in the plate/shell layer domain Ω (see the mentioned works for details). The plate/shell geometry is rectangular (a and b are their lengths in the $x(-\alpha)$ and $y(-\beta)$ directions, respectively) on Ω; their edges are simply supported while the layer exhibits orthotropic behavior in both the lamina and plate/shell reference systems, ie, cross-ply laminates are investigated. The structures are loaded by harmonic distribution of transverse pressure, applied in correspondence to the t-top surface of the N_l-layer. The amplitude is here denoted by $P^{N_l}_{zt}$.

Closed-form solutions and FEM implementations, as well as flat and curved geometries, are discussed in different subsections.

All the considered results are new elaborations of the author's previous works. While carrying out this new elaboration the author has considered most of the results reported in the literature that apply Reissner's Theorem.

7.1 Closed form solutions for plates

Table 2, reproduced from [58] is related to static bending of cross-ply plates. Layer-wise results, based on RMVT and PVD, are compared with the 3D analysis by Noor and Burton [101]. In-plane and transverse stresses and displacements are given for both cases of parabolic and linear fields for $\sigma_{\mathbf{n}}$ and $\mathbf{u}$. Two values of the thickness ratio a/h and orthotropic ratio E_L/E_T are investigated (standard notations are used to denote mechanical properties of the lamina (see, [17,21])); t, b, c (plate-top, -bottom, and -center, respectively) denote the location in the z-direction of the indicated values. The obtained results show the excellent agreement between the mixed parabolic (LM2) solutions and the 3D analysis. The transverse shear stresses, as related to RMVT applications, are those obtained *a priori*. In some cases the results related to the mixed linear (LM1) cases can be more accurate than

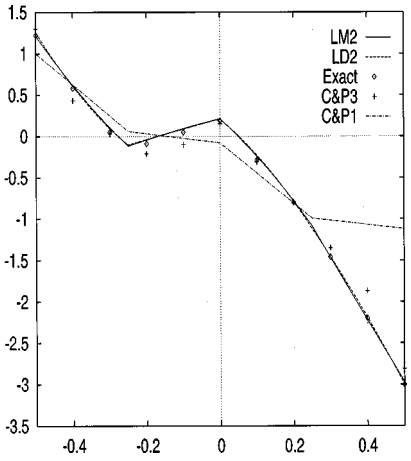

Fig. 8 Amplitude of in-plane displacement $U_z \times E_T / P_{z_t}^{N_l} h$ vs z/h. Comparison of present and other ESLM results to 3D-elasticity [32]. Antisymmetric 4-layer case, $a/h=4$. Mechanical data of the lamina: $E_L=25\times10^6$ psi, $E_T=1\times10^6$ psi, $G_{LT}=0.5\times10^6$ psi, $G_{TT}=0.2\times10^6$ psi, $\nu_{LT}=\nu_{TT}=.25$

the parabolic cases related to the displacement formulated theories (LD2); as expected, as a/h and E_L/E_T decrease, the discrepancies between the different modelings increase.

Through-the-thickness behavior of in-plane displacements and transverse stress fields are compared in Figs. 8 and 9, respectively. Layer-wise results are compared to the elasticity solution and to analyses by Cho and Parmerter [102]. Both *a priori* (LM2-M) and *a posteriori* (LM2-3D, obtained by integration of 3D indefinite equilibrium equations) transverse shear stresses are given in Fig. 9. It is made evident that RMVT furnishes a three-dimensional description of local stress and displacement fields of layered plates. It should be underlined that both displacement and transverse stresses are evaluated *a priori*, ie, there is no need to implement any post-processing procedures. C&P1 and C&P3 are the linear and cubic cases of the original ESLM theory proposed by Ambartsumian [35], Whitney [20], and Rath and Das [38].

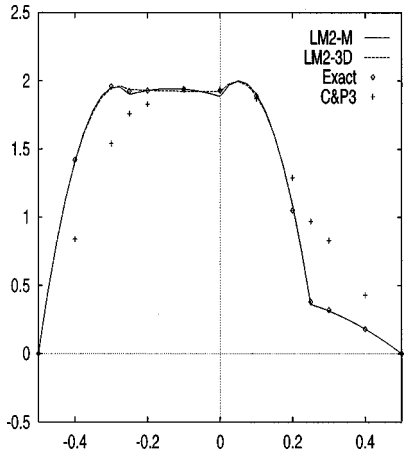

Fig. 9 Transverse shear stress amplitude $S_{xz} \times 1/P_{x_i}^{N_l}$ vs z/h; Comparison of present and other ESLM to Elasticity [32]; Antisymmetric 4 layer case, $a/h=4$; Same data as in Fig 8

Table 3. RMVT vs other results. Maximum transverse displacement $\overline{U_z}=U_z\times100E_Th^3/(P_{z_t}^{N_l}a^4)$ $(z=0)$ of thick plate in cylindrical bending. Comparison of present analyses to exact solutions by Pagano [32] and to available mixed results. Same mechanical data as in Fig. 9.

	$a/h=4$		$a/h=6$	
	$N_l=3$	$N_l=4$	$N_l=3$	$N_l=4$
Exact	2.887	4.181	1.635	2.556
C&P3	-	4.083	-	2.501
C&P1	-	3.316	-	2.107
LC&W	2.687	3.587	1.514	2.242
	RMVT results			
LM4	2.887	4.181	1.625	2.556
EMZC3	2.881	4.102	1.634	2.514
EMZC3tm	2.881	4.105	1.634	2.519
EMZC2	2.831	3.478	1.602	2.195
EMZC1	2.904	3.300	1.634	2.095
EMZC1m	2.907	3.316	1.636	2.107

Interlaminar continuous transverse shear stresses are described by Cho and Parmerter [102] while transverse normal strain-stress effects are discarded.

RMVT formulated models by Murakami [44], Toledano and Murakami [46] and Carrera [70,73] are compared to other classical analyses in Tables 3 and 4. Mostly ESLM results are given in these two Tables while a comparison between LW and ESLM implementations, based on RMVT, are compared in Table 5. The authors' initials are added to the acronyms defined in Section 4.4 for those cases in which results are not taken from Carrera's papers: for instance EMZC3tm is the EMZC3 theories formulated by Toledano and Murakami [45]; see Table 1 for a complete list of these modelings. The IK&T by Iblidi, Ka and Touratier [103] ESLM theory consists of an improved version of the original theory by Rath and Das [38], while D&S1 and D&S3 are linear and third order theories which correspond to a particular case of Rath and Das [38] models. Ren's [104] very elegant analysis, based on Lekhnitskii's works [33,34] is also quoted. The HOT by Lo, Christensen, and Wu are also compared. The considered classical models (C&P1, C&P3, D&S1, D&S3, IK&T, Ren) allow interlaminar continuous transverse shear stresses, only, and discard transverse normal

Table 4. RMVT vs other results. Influence of thickness ratio on amplitude of transverse displacement (computed in $z=0$) and amplitude of transverse shear stress (compuited in $z=0$ unless denoted). Rectangular ($b=3a$) three layered plates. Exact solution by Pagano [32]. Same mechanical data as in Fig. 8.

	$U_z\times100E_Th^3/(P_{z_t}^{N_l}a^4)$			$S_{xz}/(P_{z_t}^{N_l}a/h)$			
a/h	4	10	20	4	z	10	20
Exact	2.820	0.919	0.610	0.387	-	0.420	0.434
IK&T	2.729	0.918	0.609	0.378	-	0.441	0.451
D&S1	2.717	0.881	0.599	0.366	-	0.419	-
D&S3	2.757	0.919	0.610	0.329	-	0.420	-
Ren	2.80	0.920	-	0.317	-	0.415	-
EDZ3	2.625	0.867	0.596	0.378	−0.17	0.427	0.436
EDZ3d	2.644	0.866	0.593	0.377	0	0.427	0.436
			RMVT results				
LM4	2.821	0.919	0.610	0.387	−0.23	0.420	0.434
EMZC3	2.815	0.919	0.609	0.385	−0.23	0.420	0.434
EMZC2	2.767	0.906	0.606	0.393	−0.23	0.421	0.435
EMZC1	2.839	0.915	0.606	0.399	−0.23	0.420	0.434
EMZC3d	2.832	0.918	0.607	0.386	±0.27	0.420	0.434
EMZC2d	2.784	0.904	0.604	0.393	±0.23	0.421	0.435
EM1ZCd	2.839	0.915	0.606	0.394	±0.23	0.420	0.434

Table 5. Comparison to 3D analysis by Pagano and Hatfield [118] of RMVT results in both LW and ESLM cases. *A priori* vs *a posteriori* values of transverse shear stresses $S_{xz}\times h/P_{z_t}^{N_l}a$ evaluated at $z=0$ for three and nine layered plates. Same mechanical data as in Fig. 9.

		$N_l=3$					$N_l=9$				
	a/h	2	4	10	20	100	2	4	10	20	100
Exact		0.153	0.219	0.301	0.328	0.339	0.204	0.223	0.247	0.255	0.259
LM1	3D	0.164	0.229	0.304	0.329	0.339	0.196	0.223	0.247	0.255	0.259
	M	0.167	0.229	0.302	0.326	0.336	0.193	0.220	0.245	0.255	0.257
LM2	3D	0.154	0.219	0.301	0.328	0.339	0.204	0.223	0.247	0.255	0.259
	M	0.155	0.221	0.302	0.328	0.339	0.204	0.223	0.247	0.255	0.259
LM2	3D	0.154	0.219	0.301	0.328	0.339	0.204	0.223	0.247	0.255	0.259
	M	0.154	0.219	0.301	0.328	0.339	0.204	0.223	0.247	0.255	0.259
EMZC1	3D	0.155	0.219	0.300	0.327	0.338	0.220	0.222	0.244	0.254	0.258
	M	0.159	0.228	0.315	0.344	0.355	0.146	0.143	0.155	0.162	0.165
EMZC2	3D	0.153	0.219	0.302	0.328	0.338	0.221	0.221	0.244	0.254	0.259
	M	0.147	0.217	0.303	0.331	0.342	0.125	0.138	0.156	0.163	0.167
EMZC3	3D	0.149	0.217	0.301	0.328	0.339	0.190	0.221	0.246	0.255	0.259
	M	0.157	0.225	0.310	0.339	0.350	0.197	0.232	0.259	0.269	0.273

stresses effects. These types of classical theories have experienced difficulties in including σ_{zz} effects. Such effects have only been included in very recent works by Aitharasu and Averill [39]. From this point of view, RMVT does not present any difficulties to include transverse shear and normal stresses. σ_{zz} was in fact retained in the RMVT theory already by Toledano and Murakami [45]. Mixed results, discarding σ_{zz}, have also been implemented to show the effects of σ_{zz}; these are denoted by adding the suffix $-$d to the correspondent acronyms. The given results show that RMVT analysis, retaining σ_{zz}, leads to the best ESLM descriptions. These comments are further confirmed by comparing EMZC3d, EMZC2d, EMZC1d to EMZC3, EMZC2, EMZC1 analyses. Nevertheless, EDZ3 results show that the classical displacement formulation can be greatly improved by introducing a zigzag function $(-1)^k\boldsymbol{u}_Z$. It is of interest to notice that the accuracy of ESLM analysis is very much subordinate of the the order of the expansion used for the displacement and/or stress fields. Layer-wise LM4 always coincides with the elasticity solution. Some insights on the comparison between ESLM and LW formulated theories are given in Table 5. Transverse shear stresses, evaluated a priori (denoted by M), are compared to those obtained by the integration of the 3D indefinite equilibrium equation (denoted by 3D) are compared for a three layered and a nine layered plate. Very thick $(a/h=2)$ and thin $(a/h=100)$ plates are analyzed. Layer-wise analysis matches the exact solution for all values of the considered thickness ratios with excellent accuracy. Such an accuracy is confirmed for both symmetrically and unsymmetrically laminated plates. Furthermore, the convergence rate related to the increasing order in the expansion used for $\boldsymbol{u}^k$ and $\boldsymbol{\sigma}_n^k$ increases by the number of layers N_l increasing. Quite different behavior has to be registered for ESLM results. EMZC1 and EMZC2 work better for symmetrically laminated plates. EMZC2 and EMZC3 results show the effectiveness of parabolic terms in the $\boldsymbol{u}$ expansion for unsymmetrically laminated plate analysis. ESLM *a priori* descriptions of transverse stresses related to decreasing a/h, are poorer than those obtained *a posteriori*. *A priori* descriptions of transverse stresses remain excellent in layer-wise cases. More comprehensive comparisons between RMVT and classical theories are given in Tables 6 and 7. Static and dynamic problems are addressed. More than forty theories are compared in Table 7. The suffix *ni*, which is introduced in these tables, denotes particular case theories in which homogeneous top-bottom transverse shear stress conditions are not imposed. The influence of the shear correction factor χ has

Table 6. In-plane and out-of-plane stress amplitudes. Simply supported square plates $a/h=5$. Cross-ply skew-symmetric and symmetric laminates as in Table 1. $E_L/E_T=30$, $G_{LT}/E_T=G_{Lz}/E_T=.50$, $G_{TT}/E_T=.35$, $\nu_{LT}=\nu_{Lz}=.3$, $\nu_{TT}=0.49$.

	0/90/0			0/90/0/90		
z	$\sigma_{xx}/P_{z_t}^{N_l}$ $+.5$	$\sigma_{xz}/P_{z_t}^{N_l}$ 0	$\sigma_{zz}/P_{z_t}^{N_l}$ 0	$\sigma_{xx}/P_{z_t}^{N_l}$ $-.5$	$\sigma_{xz}/P_{z_t}^{N_l}$ 0	$\sigma_{zz}/P_{z_t}^{N_l}$ 0
			Classical analysis			
LD4	15.52	1.374	0.4982	−15.02	1.293	0.4955
LD3	15.52	1.373	0.4982	−15.02	1.293	0.4955
LD2	15.33	1.357	0.4982	−14.99	1.290	0.4954
LD1	14.27	1.369	0.4945	−13.86	1.301	0.4952
EDZ3	15.69	1.357	0.4973	−14.70	1.307	0.4955
EDZ2	14.28	1.367	0.4999	−11.16	1.356	0.4953
EDZ1	13.85	1.363	0.4808	−12.62	1.386	0.4839
EDZ3d	15.31	1.354	0.5000	−14.85	1.314	0.5000
EDZ2d	14.14	1.363	0.5000	−11.29	1.368	0.5000
EDZ1d	14.14	1.363	0.5000	−12.61	1.391	0.5000
ED4	15.39	1.366	0.4977	−15.05	1.307	0.4953
ED3	15.51	1.360	0.4978	−14.22	1.325	0.4959
ED2	11.35	1.447	0.4977	−10.80	1.375	0.4956
ED1	10.98	1.443	0.4840	−12.25	1.385	0.4839
ED4d	15.36	1.358	0.5000	−15.30	1.320	0.5000
ED3d	15.36	1.358	0.5000	−14.38	1.345	0.5000
ED2d	11.17	1.443	0.5000	−10.93	1.395	0.5000
ED1d	11.17	1.443	0.5000	−12.22	1.402	0.5000
			RMVT results			
LM4	15.52	1.374	0.4987	−15.02	1.293	0.4956
LM3	15.35	1.374	0.4987	−14.86	1.293	0.4985
LM2	15.03	1.375	0.5250	−14.59	1.294	0.5078
LM1	10.29	1.723	0.5843	−9.046	1.437	0.6477
LM4ni	15.52	1.374	0.4984	−15.02	1.293	0.4955
LM3ni	15.52	1.373	0.4984	−15.02	1.293	0.4954
LM2ni	15.43	1.367	0.5023	−15.00	1.293	0.4970
LM1ni	15.54	1.386	0.5030	−14.50	1.301	0.4937
EMZC3	15.71	1.358	0.4984	−14.67	1.307	0.4938
EMZC2	14.27	1.370	0.5096	−11.02	1.356	0.5129
EMZC1	13.86	1.362	0.5043	−12.61	1.386	0.5157
EMZC3d	15.28	1.355	0.5012	−14.81	1.313	0.4987
EMZC2d	14.12	1.367	0.5092	−11.15	1.367	0.5180
EMZC1d	14.17	1.363	0.5241	−12.60	1.391	0.5320
EMZC3ni	15.75	1.358	0.4982	−14.71	1.308	0.4953
EMZC2ni	14.48	1.369	0.5010	−11.17	1.356	0.4943
EMZC1ni	14.14	1.366	0.4814	−12.58	1.388	0.4848
EMC4	15.40	1.366	0.4968	−15.21	1.305	0.4941
EMC3	15.46	1.362	0.4983	−14.13	1.324	0.4973
EMC2	11.25	1.436	0.5309	−10.15	1.373	0.5287
EMC1	10.32	1.373	0.6121	−12.26	1.386	0.5855

Table 7. Circular frequency parameter $\omega h\sqrt{\rho/E_T}$ of simply supported square plates. Data: $a/h=5$; Cross-ply skew-symmetric and symmetric laminates (the total thickness of layers 90° degree oriented is the same of those 0° degree oriented); $G_{LT}/E_T = G_{Lz}/E_T = .50$, $G_{TT}/E_T = .35$, $\nu_{LT} = \nu_{Lz} = .3$, $\nu_{TT} = 0.49$. 3D solution given by Noor and Burton [101].

N_l	2		10		3		9	
$\frac{E_t}{E_T}$	3	30	3	30	3	30	3	30
3D	0.2392	0.3117	0.2530	0.4027	0.2516	0.3739	0.2535	0.4040
Classical analysis								
K& K	0.2388	0.3117	0.2527	0.4028	-	-	0.2536	0.4027
FSDT	0.2379	0.3165	0.2527	0.4086	-	-	0.2531	0.4067
LD4	0.2392	0.3117	0.2530	0.4027	0.2516	0.3739	0.2535	0.4040
LD3	0.2392	0.3117	0.2530	0.4027	0.2516	0.3739	0.2535	0.4040
LD2	0.2395	0.3168	0.2530	0.4027	0.2517	0.3763	0.2535	0.4040
LD1	0.2478	0.3210	0.2534	0.4042	0.2556	0.3808	0.2540	0.4058
EDZ3	0.2392	0.3156	0.2532	0.4042	0.2517	0.3761	0.2536	0.4058
EDZ2	0.2418	0.3180	0.2568	0.4250	0.2527	0.3803	0.2570	0.4254
EDZ1	0.2478	0.3210	0.2767	0.4305	0.2717	0.3842	0.2772	0.4286
EDZ3d	0.2610	0.3261	0.2713	0.4064	0.2700	0.3795	0.2717	0.4074
EDZ2d	0.2659	0.3300	0.2772	0.4285	0.2717	0.3842	0.2772	0.4286
EDZ1d	0.2659	0.3300	0.2773	0.4306	0.2717	0.3842	0.2772	0.4286
ED4	0.2394	0.3133	0.2539	0.4078	0.2518	0.3764	0.2544	0.4093
ED3	0.2394	0.3167	0.2540	0.4080	0.2519	0.3766	0.2545	0.4095
ED2	0.2418	0.3198	0.2540	0.4291	0.2569	0.4031	0.2581	0.4308
ED1	0.2662	0.3367	0.2540	0.4340	0.2778	0.4082	0.2787	0.4343
ED4d	0.2612	0.3241	0.2540	0.4102	0.2703	0.3800	0.2727	0.4116
ED3d	0.2613	0.3269	0.2723	0.4102	0.2703	0.3800	0.2727	0.4116
ED2d	0.2659	0.3316	0.2783	0.4327	0.2778	0.4082	0.2787	0.4343
ED1d	0.2662	0.3367	0.2783	0.4340	0.2778	0.4082	0.2787	0.4343
ED1d$^{\chi=5/6}$	0.2610	0.3264	0.2723	0.4118	0.2717	0.3871	0.2726	0.4118
ED1d$^{\chi=2/3}$	0.2537	0.3123	0.2640	0.3839	0.2632	0.3613	0.2642	0.3838
CLT	0.2972	0.4066	0.3150	0.6435	0.3157	0.6519	0.3157	0.6519
RMVT results								
LM4	0.2392	0.3117	0.2530	0.4027	0.2516	0.3739	0.2535	0.4040
LM3	0.2392	0.3115	0.2530	0.4027	0.2516	0.3739	0.2535	0.4040
LM2	0.2392	0.3115	0.2530	0.4027	0.2516	0.3738	0.2525	0.4040
LM1	0.2312	0.2354	0.2527	0.4011	0.2466	0.3354	0.2532	0.4019
LM4ni	0.2392	0.3117	0.2530	0.4027	0.2516	0.3739	0.2535	0.4040
LM3ni	0.2392	0.3117	0.2530	0.4027	0.2516	0.3739	0.2535	0.4040
LM2ni	0.2394	0.3143	0.2530	0.4027	0.2517	0.3749	0.2535	0.4040
LM1ni	0.2417	0.3134	0.2530	0.4031	0.2511	0.3721	0.2535	0.4044
EMZC3	0.2392	0.3144	0.2531	0.4042	0.2517	0.3758	0.2536	0.4052
EMZC2	0.2408	0.3133	0.2565	0.4035	0.2523	0.3782	0.2578	0.4242
EMZC1	0.2436	0.3131	0.2758	0.4276	0.2701	0.3789	0.2765	0.4260
EMZC3d	0.2610	0.3251	0.2713	0.4063	0.2700	0.3793	0.2717	0.4073
EMZC2d	0.2641	0.3247	0.2768	0.4269	0.2711	0.3819	0.2769	0.4273
EMZC1d	0.2625	0.3223	0.2766	0.4277	0.2701	0.3789	0.2765	0.4260
EMZC3ni	0.2392	0.3151	0.2531	0.4042	0.2517	0.3758	0.2535	0.4053
EMZC2ni	0.2418	0.3169	0.2568	0.4250	0.2525	0.3791	0.2570	0.4252
EMZC1ni	0.2455	0.3181	0.2766	0.4305	0.2711	0.3822	0.2771	0.4284
EMC4	0.2393	0.3129	0.2539	0.4075	0.2518	0.3739	0.2771	0.4089
EMC3	0.2393	0.3141	0.2538	0.4072	0.2518	0.3739	0.2543	0.4087
EMC2	0.2400	0.3117	0.2570	0.4258	0.2555	0.3739	0.2575	0.4275
EMC1	0.2566	0.3179	0.2754	0.4230	0.2700	0.3354	0.2756	0.4224

also been considered in Table 7 (ED1d$^{\chi=5/6}$ and ED1d$^{\chi=2/3}$). The following main comments and remarks can be made on the reported analysis.

- LWM descriptions are more accurate than corresponding ESLM ones;
- Descriptions based on RMVT are more accurate than the corresponding formulations based on PVD;
- EM cases are much more accurate than ED ones, in other words, RMVT is much more effective for ESLM formulations;
- RMVT analyses do not require any post=processing procedures;
- LWM are computationally expensive compared to ESL theories; on the other hand, the use of a layer-wise description is essential for those cases in which an accurate description of σ_{zz} and any related effects is required. In other words, E type theories experience difficulties in describing σ_{zz} effects.

Further, minor comments are here listed.

- N_l increasing, the results of LWM theories become independent by the order N used, or by RMVT or PVD implementions. This is caused by the intrinsic increment of the number of degrees of freedom.
- The order of the expansion N used plays a very important role, especially as far as unsymmetric laminates are concerned. Note that the quadratic expansions are much more effective for unsymmetric laminates. For N increasing the differences between LM and LD disappear.
- The accuracy of the classical ED type results decreases with the increase of N_l.

Table 8. Influence of thickness ratio on the accuracy of the considered theories. Cylindrical bending of thermally loaded plates problem considered by Bhaskar *et al.* [105]; three layered plate 0°/90°/0°. In-plane displacement $U_x/(\alpha_L T_0 a)$ at $z=\mp h/2$. Mechanical data of the lamina: $E_L/E_T=25$, $G_{LT}/E_T=.5$, $G_{TT}/E_T=.2$, $\nu_{LT}=\nu_{TT}=.25$, $\alpha_T/\alpha_L=1125$.

a/h	2	4	10	20	50	100
Exact	±13.38	±7.470	±5.009	±4.589	±4.467	±4.449
Classical analysis						
LD4	±13.37	±7.469	±5.009	±4.589	±4.467	±4.449
LD3	±13.28	±7.467	±5.009	±4.589	±4.467	±4.449
LD2	±12.35	±7.345	±5.001	±4.587	±4.467	±4.449
LD1	±7.327	±6.136	±5.311	±5.147	±5.099	±5.092
EDZ3	±12.83	±7.416	±5.046	±4.588	±4.467	±4.449
EDZ2	±6.202	±5.268	±4.617	±4.489	±4.451	±4.445
EDZ1	±4.263	±5.581	±6.494	±6.674	±6.728	±6.736
ED4	±12.21	±7.570	±5.044	±4.598	±4.468	±4.449
ED3	±12.22	±7.566	±5.044	±4.598	±4.468	±4.450
ED2	±4.531	±4.465	±4.447	±4.445	±4.444	±4.443
ED1	±10.59	±10.59	±10.59	±10.59	±10.59	±10.59
CLT	±4.444	±4.444	±4.444	±4.444	±4.444	±4.444
RMVT analysis						
LM4	±13.37	±7.461	±5.009	±4.589	±4.467	±4.449
LM3	±11.62	±7.169	±5.975	±4.581	±4.466	±4.449
LM2	±10.13	±7.116	±5.015	±4.594	±4.466	±4.449
LM1	±8.686	±6.760	±5.057	±4.675	±4.558	±4.540
EMZC3	±12.46	±7.388	±5.007	±4.589	±4.467	±4.449
EMZC2	±5.994	±5.192	±4.606	±4.486	±4.450	±4.450
EMZC1	±4.374	±5.587	±6.488	±6.673	±6.728	±6.736
EMC4	±11.32	±7.374	±5.025	±4.594	±4.468	±4.449
EMC3	±10.96	±7.281	±5.015	±4.592	±4.468	±4.450
EMC2	±4.489	±4.454	±4.445	±4.444	±4.444	±4.443
EMC1	±6.739	±6.739	±6.739	±6.739	±6.739	±6.739

Table 9. Comparison of present analyses to 3D Exact solutions by Ren [37]. Case *a*. Single layer 90°. Transverse displacement and transverse shear stress amplitude.

R_β/h	2	4	10	50	100
		$U_z \times \frac{10 E_T h^3}{P^1_{z_b} R^4_\beta},\ z=0$			
Exact	0.9986	0.312	0.115	0.077	0.0755
Classical analysis					
CLT	0.0764	0.0752	0.0749	0.0748	0.0748
D&P	0.803	0.278	0.108	0.0762	0.0751
LM2	1.094	0.3219	0.1151	0.0770	0.0755
$LM2^2$	1.030	0.3140	0.1147	0.0770	0.0755
$LM2^5$	1.000	0.3121	0.1146	0.0770	0.0755
$LM1^2$	1.183	0.3466	0.1190	0.0771	0.0756
$LM1^5$	0.9727	0.3097	0.1156	0.0770	0.0755
RMVT results					
LD2	0.8905	0.2778	0.1087	0.0.767	0.0.755
$LD2^2$	0.9628	0.3071	0.1142	0.0770	0.0755
$LD2^5$	0.9940	0.3117	0.1146	0.0770	0.0755
LD1	0.9104	0.2793	0.1085	0.0764	0.0752
$LD1^2$	0.8787	0.2773	0.1087	0.0767	0.0754
$LD1^5$	0.9606	0.3040	0.1134	0.0770	0.0755
		$\left\lvert S_{\beta z} \times \frac{h}{P^1_{z_b} R_\beta} \right\rvert,\ z=0$			
Exact	0.555	0.572	0.579	0.568	0.565
RMVT results					
LM2	0.7031	0.6328	0.5906	0.5681	0.5653
$LM2^3$	0.4614	0.5295	0.5699	0.5673	0.5661
$LM2^5$	0.5673	0.5715	0.5796	0.5677	0.5652

- The use of the zig-zag function improves very much the results of related classical displacement formulations. In fact, EDZ analyses are more accurate than ED ones. Advantages also occur by imposing interlaminar continuity, ie, EM results are more accurate than ED ones.
- σ_{zz} can play a predominant role. For instance EMZC3d results can be much worse than EMZC1 ones. σ_{zz} is very much influenced by a/h. Thick plates show that σ_{zz} leads to an unsymmetrical through-the-thickness distribution of local parameters. Such unsymmetry cannot be described by any two-dimensional theory that neglects σ_{zz}. As pointed out by Koiter KR, one underlines that the order of magnitude of σ_{zz} is the same as that of the transverse shear stresses.
- When increasing N and/or N_l the fulfillment of homogeneous conditions at the top-bottom plate surfaces on transverse stresses in LM and EM type theories becomes irrelevant. Note that these conditions cannot be imposed in LM1 cases where only top and bottom stress variables are used: to force them would signify neglecting stiffnesses and/or compliance of the top and bottom layers.
- The use of shear correction factor χ is questionable. As demonstrated (see [100]), the correct value of shear correction, being related to the form of the distribution of shear stresses, is problem dependent. It can happen that a shear corrected theory which neglects σ_{zz} can lead to better results than the analysis in which such a stress is preserved. Furthermore, shear correction factors can only improve global response but they are completely ineffective to improve local response.

Thermal cases are considered in Table 8. Classical and RMVT analyses are compared. The analyses presented refer to a thermomechanical problem for which the three-dimensional exact solution has recently been given by Bhaskar, Varadan, and Ali [105]. A cylindrically bent plate, loaded by a temperature field given by $T=T_0 2z/h \sin \pi x/a$, is considered. α_L and α_T are the thermal expansion coefficients in the longitudinal and transverse fiber directions. RMVT is confirmed as being a suitable tool to analyze thermo-mechanical problems. The comments made for the mechanical loading cases are confirmed. In addition one should note that LM1 and LD1 linear cases can be very inaccurate, even though thin plates are considered. This phenomenon is basically due to the fact that the considered temperature loading exhibits a linear z-distribution in the plate. As a consequence, the related transverse normal thermal strains are linear. Such a linear distribution requires at least a quadratic transverse displacement field u_z in each-layer, which is not considered by LM1 or by LD1 analyses. Such inaccuracy is much more evident for the ESL-type analyses. CLT analysis, which neglects any transverse normal strains effect, matches the exact solution of thin plates. This does not happen for the EMZC1, EMC1, EDZ1, ED1. In fact, the linear transverse displacement fields u_z related to the latter cases, force a constant, non-physical distribution of transverse strains that causes errors, even though thin plates are analyzed, (see [75] for more information).

7.2 Closed form solutions for shells

Closed form solutions related to cylindrical shell problems are discussed in Tables 9 and 10 and Figs. 10–12. Analyses presented by Jing and Tzeng [78], Bhaskar and Varadan [76] and Carrera [60] are used. Figures 9 and 10 compare RMVT applications and classical models to exact 3D solutions.

Table 10. Effect of radii to length ratio R/a on $\omega \times a^2\sqrt{\rho/h^2E_T}$. Comparison to exact solution by Ye and Soldatos [108] and to other refined analyses. $a/h=10$, $m=1$, $n=2$ unless given in brackets. Three layered ringed shell 0/90/0, $h_1=h_3=h_2/2$.

R_β/a	5	10	50	100
Exact	10.305^{14}	10.027^{22}	9.834^{24}	9.815
		Classical analysis		
PAR_{ds}	10.496	10.223	10.032^{26}	10.013
HYP_{ds}	10.496	10.226	10.036^{26}	10.018
UNI_{cs}	10.462	10.187	9.996^{28}	9.977
PAR_{cs}	10.329	10.051	9.859^{26}	9.840
HYP_{cs}	10.328	10.050	9.858^{26}	9.839
ZZL	10.462^{14}	10.187^{24}	9.996^{16}	9.971^{4}
EDZ3	10.453^{14}	10.179^{22}	9.988^{26}	9.969
EDZ3d	10.470^{14}	10.193^{22}	9.998^{26}	9.979
EDZ1	11.318^{14}	11.063^{20}	10.879^{20}	10.862
EDZ1d	11.318^{14}	11.064^{20}	10.880^{20}	10.862
		RMVT analysis		
LM4	10.305^{14}	10.027^{22}	9.834^{26}	9.815
EMZC3	10.309^{14}	10.030^{22}	9.837^{26}	9.818
EMZC3d	10.324^{14}	10.043^{22}	9.847^{26}	9.828
EMZC1	10.328^{14}	10.046^{22}	9.850^{26}	9.831
EMZC1d	10.328^{14}	10.046^{22}	9.850^{26}	9.831

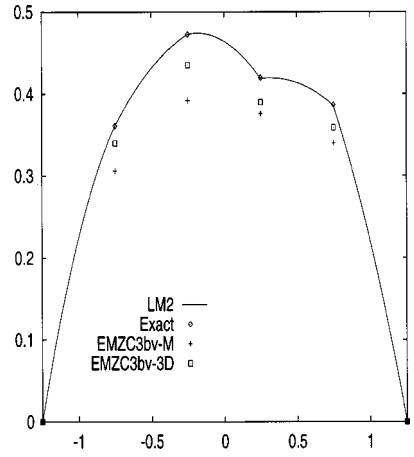

Fig. 11 Amplitude of transverse shear stress $|S_{\alpha z}\times 10h/P^1_{z_b}R_\beta|$ vs z; Varadan and Bhaskar's cylindrical shells with $R_\beta/h=4$; Five layer case

Mixed analyses by Jing and Tzeng [78] and by Carrera [60] are used in Fig. 9 and Table 9 and compared to the 3D elasticity solution by Ren [37] and are related to cross-ply laminated, cylindrical panels in cylindrical bending. The case of a transverse pressure applied to the top (external $p^{N_l}_{z_t}=\Sigma_n P^{N_l}_{z_t}\sin n\pi\beta/b$) layer has been considered. The geometrical data are: $n=1$, $R_\beta/b=\pi/3$ (n is the number of circumferential waves and R_β is the radius of the cylindrical panel, see Appendix B). while the mechanical data are, $E_L=25\times 10^6$ psi (172 GPa), $E_T=10^6$ psi (6.9 GPa), $G_{LT}=.5\times 10^6$ psi (3.4 GPa), $G_{TT}=.2\times 10^6$ psi (1.4 GPa), $\upsilon_{LT}=\upsilon_{TT}=0.25$. Figures 10 and 11 are related to the shell problems treated by Varadan and Bhaskar [106] who gave exact solutions for cross-ply laminated, cylindrical shells, subjected to transverse pressure at the bottom internal surface $p^1_{z_b}=\Sigma_{m,n}P^1_{z_b}(\sin m\pi\alpha/a)(\sin n\pi\beta/b)$ (m is the number of waves in the α-direction). The geometrical data are: $a/R_\beta=4$, $m=1$, $n=8$. The D&P theory [107] fulfills the homogeneous conditions for the transverse shear stresses. A single layer case is consider in Table 9. Transverse displacement and transverse shear stress values are compared. CLT solutions are also taken from [37]. Five different thickness ratios have been investigated. The layer-wise analysis implements fictitious interfaces. For the one-layer case, the mixed solution has been restricted to the parabolic transverse stress and displacement expansions. In the case of a multilayered shell, top-bottom homogeneous conditions for the transverse shear stress could not be imposed for the linear expansion. Their linkage would, in fact, require discarding the stiffness and/or compliance contributions related to the top and bottom shell layers. These conditions have therefore not been considered in all the quoted LM1 results. The following comments can be made which mostly confirm the conclusion given for the plate cases:

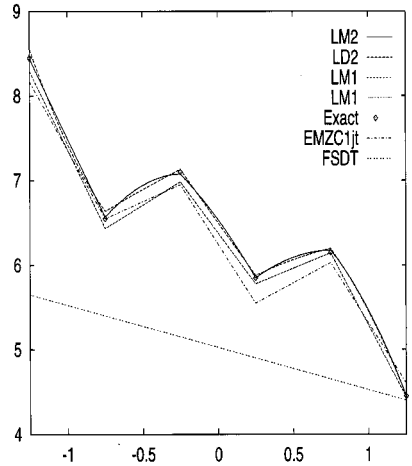

Fig. 10 Amplitude of in-plane displacements $U_\beta \times 100E_Th^2/P^{N_l}_{z_t}R^3_\beta$ vs z; Ren's cylindrical panel with $R_\beta/h=4$; Five layer case

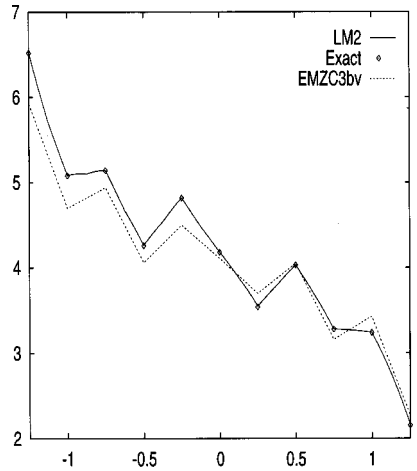

Fig. 12 Amplitude of in-plane displacemnets $U_\beta \times 10E_Lh^2/P^1_{z_b}R^3_\beta$ vs z; Varadan and Bhaskar's cylindrical shells with $R_\beta/h=4$; Ten layer case

- Excellent agreement between LM2 and exact results has been found for both displacement and transverse stresses even though very thick panels were considered. A better description than the related layer-wise analyses, based on displacement formulations, should be registered.
- An acceptable convergence rate of the layer-wise model has been found for thick shells. Due to the other approximations concerning curvature terms, such a rate is slower than those found for the plate cases.
- For the one-layer-case LM2, LD2, LD1 are equivalent to the ESLM results. Approximations related to curvature effects are more evident in this case.
- LD1 analysis can lead to a better description of the deflections with respect to the LD2 cases. This unexpected result should be considered as being due to the fact that a local value is concerned.
- The accuracy of the LW results is independent of the lamination scheme.
- Results related to different theories merge for thin shells.

It is of a certain interest to notice that stress and displacement formulations lead to a lower and higher estimation of the shell stiffness, as far as exact-3D solutions are concerned. LD2 and LD1 displacement values are in fact always lower than the exact ones. In the mixed cases, a simple conclusion cannot be drawn: this very much depends on the relative role played by the in-plane and out-of-plane energy, and the results obviously become problem dependent. For most of the considered problems, it has been found that mixed and displacement solutions lead to higher and lower approximations for the displacements, respectively.

Further comparisons of RMVT analyses to recent exact solutions by Ye and Soldatos [108] and to several refined models quoted by Timarci and Soldatos [109] has been provided in Table 10. A three-layered, moderately thick cylindrical shell has been considered. A good agreement between present mixed analysis and exact solutions has to be noticed. Better results have been found compared to standard classical displacement formulation. The value quoted in brackets, accompanying some of the numerical results in Table 10, indicates the circumferential wave number, for which the fundamental frequency was obtained. All the theories considered in [109] neglect transverse normal stress effects. Uniform UNI, parabolic PAR, and hyperbolic HYP transverse shear stress distributions in the thickness shell direction were considered, as well as two cases of interlaminar discontinuous $_{d_s}$ and continuous $_{c_s}$ shear stresses (see [109], for further details). Uniform distribution cases do not fulfill static conditions at the top and bottom shell surfaces. The *ZZL* results refer to [110], the same analysis as that of UNI_{cs}. The fundamental mode can be erroneously predicted by appropriate analysis. The importance of fulfilling the interlaminar transverse shear stress continuity, along with the advantage of using RMVT, has been confirmed by the reported analysis.

7.3 Finite element solutions for plates and shells

This section shows that RMVT is an effective tool for developing finite elements and that resulting mixed finite elements possess the same computation reliability and robustness as the classical finite elements usually employed for the analysis of single-layer, isotropic structures.

Finite element solutions based on RMVT are considered in Tables 11–13 and Figs. 13–15. Tables 11 and 12 use the same notations and acronyms employed in the previous sections. The finite element results by Rao and Meyer-Piening [62] and those recently obtained by Carrera and Demasi [73–75] are reported. Comparison to fully mixed [111], hybrid ([112], [79]), classical [26], and elasticity solutions are given. The good performance exhibited by the closed form solutions are confirmed for finite element implementations. Of particular, practical, interest is the finite element discussed in Table 13 and Figs. 13-14. The literature (see, [113] as an example), has shown that a reliable finite element for plate and shell analysis, in both linear and nonlinear problems, should belong to the Reissner-Mindlin type model. As main properties, these elements have only physical variables, displacement or rotations, as nodal variables. Associated shear locking mechanisms are contrasted by the use of mixed interpolation of tensorial components as described in Bathe and Dvorkin [113]. Many finite elements have been proposed for plates and shells (see the review articles mentioned in Section 2). Those papers which do not violate IC for transverse shear and include ZZ for the in-plane displacement components (which are mainly based on Ambartsumian [35] type approach), show the derivatives of the transverse displacements as nodal variables. In conclusion, resulting finite plate/shell elements do not meet the computational requirements listed by Bathe and Dvorkin [113]. RMVT, by means of the WFHL described in Section 5, permits one to refine the original Reissner-Mindlin plate/shell finite element formulation by Bathe and Dvorkin to multilayer structures through the inclusion of IC and ZZ. The resulting element was refereed to by Carrera [64] as RMZC (Reissner-Mindlin Zigzag-interlaminar Continuity). Such RMZC elements have successfully been applied to plate and shell geometries, static and dynamic cases, and linear and nonlinear problems. Figures 13 and 14 show some results related to nonlinear static and dynamic analysis of plates. RMZC elements are compared to FSDT and CLT. Figure 13 plots postbuckling for thick compressed orthotropic plates; λ is a load parameter applied to a reference loading vector applied to two opposite plate edges (the magnitude is $P_{axial}=1.$). A transverse disturbance loading is also applied to the plate center in order to start the postbuckling path ($P_{transverse}=.1P_{axial}$, (see, [82] for details). Figure 14 plots the linear and nonlinear dynamic response of transversely loaded anisotropic plates. ω_e is the frequency of the applied harmonic forces and w_1 and w_2 are the values of the parameters used in the employed time-integration Newmark scheme (see [82], for details).

Shell results of RMZC implementation, taken by Brank and Carrera [87], are given in Table 13 and Fig. 14. The good performance exhibited for plate geometries are confirmed for the shell cases.

Table 11. Comparison between RMVT finite element analyses and results from literature. Simply supported square plate problem, as in Pagano [119] $a/h=10$, analyzed by a 5×5 mesh nine node plate elements

	$\sigma_{xx}\times\frac{1}{p_z(a/h)^2}$	$\sigma_{yy}\times\frac{1}{p_z(a/h)^2}$	$\sigma_{zx}\times\frac{1}{p_z(a/h)}$	$\sigma_{zy}\times\frac{1}{p_z(a/h)}$	$U_z\times\frac{\cdot100\cdot h^3\cdot E_2}{P^{N_l}_{z_t}\cdot a^4}$
	$\frac{a}{2},\frac{a}{2},\pm\frac{h}{2}$	$\frac{a}{2},\frac{a}{2},\pm\frac{h}{6}$	$0,\frac{a}{2},0$	$\frac{a}{2},0,0$	$\frac{a}{2},\frac{a}{2},0$
3D (Pagano, 1970)	0.590 −0.590	0.285 −0.288	0.357	0.1228	0.7530
		Full mixed and hybrid FEM analysis			
Liou & Sun (1987)	0.580 −0.580	0.285 −0.289	0.367	0.127	0.7546
Moriya (1986)	0.5759 −0.5785	0.2820 −0.2890	0.3993	0.1296	0.7512
		Classical FEM analysis			
LD4	0.5801 −0.5784	0.2796 −0.2831	0.3724	0.1623	0.7528
LD1	0.5608 −0.5598	0.2740 −0.2776	0.3726	0.1338	0.7371
EDZ3	0.5856 −0.5825	−0.2834 −0.2828	0.3879	0.1491	0.7634
EDZ1	0.5642 −0.5625	0.2762 −0.2757	0.3777	0.1408	0.7417
ED4	0.5776 −0.5753	0.2694 −0.2692	0.2948	0.1464	0.7268
ED1	0.5113 −0.5096	0.2382 −0.2376	0.1538	0.1117	0.6313
Reddy (1984)	0.5684 -	-	0.1033	-	0.7125
		RMVT analysis			
LM4	0.5801 −0.5784	0.2796 −0.2831	0.3626	0.1249	0.7528
LM1	0.5760 −0.5748	0.2525 −0.2562	0.3615	0.0937	0.7500
EMZC3	0.5856 −0.5826	0.2829 −0.2823	0.3884	0.1270	0.7634
EMZC1	0.5674 −0.5658	0.2747 −0.2741	0.3986	0.1546	0.7442
EM4	0.5787 −0.5764	0.2708 −0.2706	0.3118	0.1259	0.7313
EM1	0.5106 −0.5090	0.2411 −0.2406	0.1979	0.0723	0.6449
Jing & Liao (1989)	0.5884 −0.5879	0.2834 −0.2873	0.3627	0.1284	0.7531

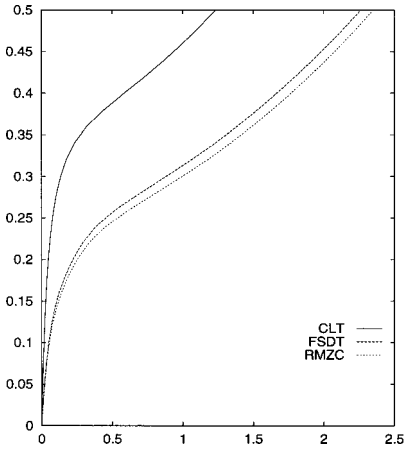

Fig. 13 Postbuckling of a compressed plate: Load parameter vs plate defection at the center; Comparisons among RMZC and classical theories. $a=10$, $h=1$; mesh 4×4. 0°/90°/0°/90°/0°, $E_L/E_T=40$, $G_{LT}/E_T=.5$, $G_{TT}/E_T=.35$, $\nu_{LT}=\nu_{TT}=.3$.

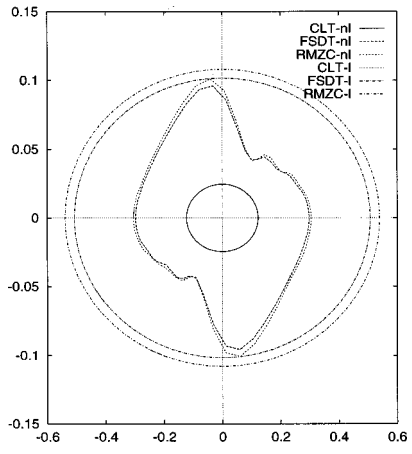

Fig. 14 Phase diagram corresponding to the steady-state-solution: $\dot{u}_z vs u_z$; Comparison between linear and nonlinear analysis for RMZC, FSDT and CLT results. $a=10$, $h=1$, mesh 4×4; 45°/−45°/45°/−45°/45°; Mechanical data as Fig. 13; $P_z(5,5)=1$; $\omega_e=0.2$; $w_1=0.535$, $w_2=0.534$

Table 12. Comparison between present analyses to exact three dimensional analysis by Pagano [119]. Mesh is made by 5×5 nine noded elements. $a/h=2$ case

	$\sigma_{xx}\times\frac{1}{p_z(a/h)^2}$	$\sigma_{yy}\times\frac{1}{p_z(a/h)^2}$	$\sigma_{zx}\times\frac{1}{p_x(a/h)}$	$\sigma_{xy}\times\frac{1}{p_z(a/h)}$	$U_z\times\frac{\cdot 100\cdot h^3\cdot E_2}{P_{z_t}^{N_l}\cdot a^4}$
	$\frac{a}{2},\frac{b}{2},\pm 1$	$\frac{a}{2},\frac{b}{2},\pm 1$	$0,\frac{b}{2},0$	$\frac{a}{2},0,0$	$\frac{a}{2},\frac{b}{2},0$
$a/h=2$					
3D	3.278 −2.653	.452 −.392	.185	.139	26.0
LD3	3.2426 −2.6233	.4544 −.3834		-	22.103
ED3	3.0752 −2.5015	.4825 −.4241	-	-	21.960
		RMVT results			
LM4	3.2430 −2.6233	.4537 −.3829	.1897	.1444	22.103
LM2	3.2352 −2.6172	.4541 −.3832	.1853	.1404	22.103
EMZC3rm	2.740 −3.260	.325 −.530	.186	.139	21.3
EMZC3	3.1594 −2.5612	.5041 −.4338	.2403	.1600	23.313
EMZC2	3.1255 −2.5286	.5021 −.4319	.2489	.1648	23.298
$a/h=50$					
3D	±1.099	±.057	.323	.031	1.10
LD3	±1.0785	±.0558	-	-	.9343
ED3	±1.0706	±.0569	-	-	.9297
		RMVT results			
LM4	±1.0786	±.0559	.3287	.0312	.9343
LM2	±1.0785	±.0558	.3280	.0305	.9343
LM1	±1.0791	±.0563	.3281	.0305	.9343
EMZC3rm	±1.152	±.060	.567	.271	.93
EMZC3	±1.0714	±.0572	.4094	.1055	.9354
EMZC2	±1.0843	±.0589	.4672	.0795	.9303

8 CONCLUDING REMARKS

This article addresses issues associated with the analysis of multilayer structures. The reported theoretical derivations, along with the quoted numerical evaluations, should prove that RMVT offers a convenient way of analyzing multilayered structures. Interlaminar continuity of transverse stresses, as well as the zig-zag form of displacements in the thickness plate/shell directions, are in fact easily introduced by RMVT. In particular, RMVT does not show any complicating effects when including the fundamental effects of transverse normal stresses and strains. Furthermore, RMVT furnishes transverse stresses *a priori*; that is, post-processing procedures are not required. Results have demonstrated that RMVT permits one to obtain a three-dimensional description of stress and strain fields of multilayer structures. Computational applications, as far as the finite element method is concerned, have also been developed. The related evaluations have demonstrated that RMVT-based finite elements have the same reliability and robustness as the classical formulations, to analyze both linear and nonlinear problems, as well as static and dynamic cases. In particular, the introduced WFHL (Section 5) permits one to preserve some of the advantages of full RMVT formulated finite elements and, at the same time, to eliminate stress variables that lead to the same computational cost of classical formulations with only displacement variables. One could conclude that RMVT should be seen as the natural extension of the Principle of Virtual Displacement (PVD) to multilayer structures. RMVT, in fact, plays the same role that PVD plays in linear/nonlinear, static/dynamic, analytical/computational analyses of single-layer plate/shell structures. In addition to the already proposed applications, further developments of RMVT could be tried. WFHL could be systematically used to introduce interlaminar continuity in the weak sense, to existing finite elements formulated on the basis of only displacement unknowns. Furthermore, RMVT, in conjunction with FEM, could easily permit a simulation of delaminated zones in the structures. The case of nonhomogenous conditions for transverse stresses could also easily be introduced. In particular interlaminar loadings, such as those introduced by layers made of piezo-materials, could be described.

Table 13. Shell panel: Comparison of results for U_z $\times 10E_Lh^3/P_{zt}^{N_l}R_\beta^4$. Exact results by Ren.

R_2/h	2	4	10	50	100
Exact	1.436	0.457	0.144	0.0808	0.0787
		Analytical			
LM2	1.436	0.4582	0.1440	0.0808	0.0787
EMZC1jt	-	0.459	0.142	0.0802	0.0780
FSDT	-	0.342	0.120	0.0793	0.0780
CLT	0.0799	0.0781	0.0777	0.0776	0.0776
		FEM			
D&P	1.141	0.382	0.128	0.0796	0.0781
RMZC	1.5600	0.4656	0.1430	0.0809	0.0787
RMZ	1.4763	0.4492	0.1400	0.0808	0.0787
RMC	1.3175	0.3625	0.1226	0.0800	0.0784

ACKNOWLEDGMENTS

The author is deeply indebted to the late Professor Eric Reissner for his encouragement in the work on RMVT. Further acknowledgments are also due to the late Professor Placido Cicala for the many suggestions and criticisms given during the review process of the paper [7] where the systematic use of RMVT was first made. Further thanks are directed to the many friends who have given their encouragement and support to the author for writing this article. Among these, Professors Liviu Librescu, Hidenuri Murakami, and Kostas P Soldatos should be mentioned.

LIST OF SYMBOLS AND ACRONYMS

Symbols and acronyms that are used frequently in places distant from their definition are listed below.

Symbols

a,b,h	-	plate/shell geometrical parameters (length, width and thickness)
k	-	sub/super-script used to denote parameters related to the k-layer
N	-	order of the expansions used for transverse stresses and displacements
N_l	-	Number of constituent layers of multilayered plate/shell
x,y,z	-	coordinates of Cartesian reference systems used for plates
α, β, z	-	curvilinear coordinates of reference systems used for shells
Γ	-	boundary of Ω
Ω	-	plate/shell reference surface

Acronyms

CLT	-	Classical Lamination Theory
ESLM	-	Equivalent Single Layer Model
FEM	-	Finite Element Method
FSDT	-	First Shear Deformation Theory
HOT	-	Higher Order Theories
HTD	-	High Transverse Deformability
IC	-	Interlaminar Continuity
KR	-	Koiter's Recommendation
LWM	-	Layer-Wise Models
RMVT	-	Reissner's Mixed Variational Theorem
RMZC	-	Finite element plate/shell element by Carrera [64] and Brank and Carrera [74]
TA	-	Transverse Anisotropy
WFHL	-	Weak Form of Hooke's Law
ZZ	-	Zig-Zag effect

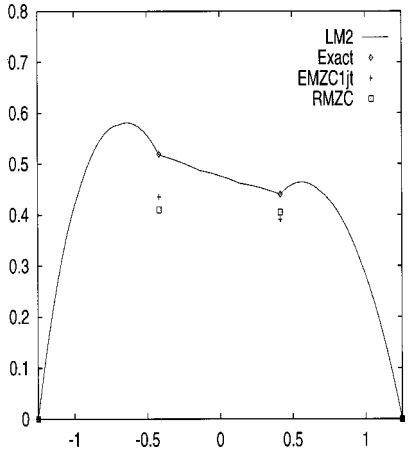

Fig. 15 Shell panel with $R_\beta/h=4$ ($h=2.5$); Transverse shear stress $\sigma_{yz}\times h/P_{zt}^{N_l}R_\beta$

APPENDIX A GOVERNING EQUATIONS FOR MULTILAYERED SHELLS

This appendix applies the RMVT to express the governing equations of a multilayered doubly curved shell in the dynamic case.

A.1 Preliminary

The salient features of the shell geometry have already been shown in Fig. 2. A laminated shell composed of N_l layers is considered. The layer geometry is denoted by the same symbols as those used for the whole multilayered shell and vice-versa. α_k and β_k are the curvilinear orthogonal coordinates (coinciding with principal curvature lines) on the layer reference surface Ω_k (middle surface of the k-layer). z_k denotes the rectilinear coordinate in the direction normal to Ω_k. Γ_k is the Ω_k boundary: Γ_k^g and Γ_k^m are those parts of Γ_k on which geometrical and mechanical boundary conditions are imposed, respectively; these boundaries are herein considered parallel to α_k or β_k. The following relations hold in the given orthogonal system of curvilinear co-ordinates for the square of line element, for the area of an infinitesimal rectangle on Ω_k, and for an infinitesimal volume, respectively [114],

$$ds_k^2=H_\alpha^k d\alpha_k^2+H_\beta^k d\beta_k^2+H_z^k dz_k^2$$

$$d\Omega_k=H_\alpha^k H_\beta^k d\alpha_k d\beta_k$$

$$dV=H_\alpha^k H_\beta^k H_z^k d\alpha_k d\beta_k dz_k \tag{31}$$

where

$$H_\alpha^k=A^k(1+z_k/R_\alpha^k),\quad H_\beta^k=B^k(1+z_k/R_\beta^k),\quad H_z^k=1.$$

R_α^k and R_β^k are the radii of curvature in the directions of α_k and β_k, respectively. A^k and B^k are the coefficients of the first fundamental form of Ω_k. For the sake of simplicity, attention is herein restricted to a shell with a constant curvature, ie, doubly curved shell (cylindrical, spherical, toroidal geometries) for which $A^k=B^k=1$.

As far as Hookes's law is concerned the formulas given in Section 4.2 are used, while the strain displacement relations for the considered geometries and within the small deformation field are [114]

$$\boldsymbol{\epsilon}_{pG}^k=\boldsymbol{D}_p\boldsymbol{u}^k+\boldsymbol{A}_p\boldsymbol{u}^k,\quad \boldsymbol{\epsilon}_{nG}^k=\boldsymbol{D}_{n\Omega}\boldsymbol{u}^k+\boldsymbol{A}_n\boldsymbol{u}^k+\boldsymbol{D}_{nz}\boldsymbol{u}^k \tag{32}$$

where

$$\boldsymbol{D}_p=\begin{bmatrix}\frac{\partial_\alpha}{H^k_\alpha} & 0 & 0\\ 0 & \frac{\partial_\beta}{H^k_\beta} & 0\\ \frac{\partial_\beta}{H^k_\beta} & \frac{\partial_\alpha}{H^k_\alpha} & 0\end{bmatrix},\quad \boldsymbol{A}_p=\begin{bmatrix}0 & 0 & \frac{1}{H^k_\alpha R^k_\alpha}\\ 0 & 0 & \frac{1}{H^k_\beta R^k_\alpha}\\ 0 & 0 & 0\end{bmatrix},$$

$$\boldsymbol{D}_{n\Omega}=\begin{bmatrix}0 & 0 & \frac{\partial_\alpha}{H^k_\alpha}\\ 0 & 0 & \frac{\partial_\beta}{H^k_\beta}\\ 0 & 0 & 0\end{bmatrix},$$

$$\boldsymbol{A}_n=\begin{bmatrix}-\frac{1}{H^k_\alpha R^k_\alpha} & 0 & 0\\ 0 & -\frac{1}{H^k_\beta R^k_\beta} & 0\\ 0 & 0 & 0\end{bmatrix},$$

$$\boldsymbol{D}_{nz}=\begin{bmatrix}\partial_z & 0 & 0\\ 0 & \partial_z & 0\\ 0 & 0 & \partial_z\end{bmatrix},$$

In order to get the strong form of governing equations, the derivative of virtual variation of displacement and stress variables must be converted, by integration by parts, to the corresponding finite variables. To do this, one finds convenience introducing the following array formulas,

$$\int_{\Omega_k}(\boldsymbol{D}_p\delta\phi)^T\varphi d\Omega_k=-\int_{\Omega_k}\delta\phi^T\boldsymbol{D}_p^T\varphi\, d\Omega_k+\int_{\Gamma_k}\boldsymbol{\delta\phi}^T\boldsymbol{I}_p^T\varphi\, d\Gamma_k$$

$$\int_{\Omega_k}(\boldsymbol{D}_{n\Omega}\delta\phi)^T\varphi d\Omega_k=-\int_{\Omega_k}\delta\phi^T\boldsymbol{D}_\Omega^T\varphi\, d\Omega_k+\int_{\Gamma_k}\delta\phi^T\boldsymbol{I}_{n\Omega}^T\varphi\, d\Gamma_k \tag{33}$$

ϕ and φ can be displacement or stress variables, respectively; while the introduced non differential arrays are:

$$\boldsymbol{I}_p=\begin{bmatrix}\frac{1}{H^k_\alpha} & 0 & 0\\ 0 & \frac{1}{H^k_\beta} & 0\\ \frac{1}{H^k_\beta} & \frac{1}{H^k_\alpha} & 0\end{bmatrix};\quad \boldsymbol{I}_{n\Omega}=\begin{bmatrix}0 & 0 & \frac{1}{H^k_\alpha}\\ 0 & 0 & \frac{1}{H^k_\beta}\\ 0 & 0 & 0\end{bmatrix}$$

The written formulas remain valid if and only if first order differential operators are involved. Upon substitution of the introduced displacement expansion, the strains are written in the following form

$$\boldsymbol{\epsilon}^k_{pG}=F_\tau\boldsymbol{D}_p\boldsymbol{u}^k_\tau+F_\tau\boldsymbol{A}_p\boldsymbol{u}^k_\tau,$$
$$\boldsymbol{\epsilon}^k_{nG}=F_\tau\boldsymbol{D}_{n\Omega}\boldsymbol{u}^k_\tau+\lambda_D F_\tau\boldsymbol{A}_n\boldsymbol{u}^k_\tau+F_{\tau_z}\boldsymbol{u}^k_\tau \tag{34}$$

where the further subscript z in F_τ denotes differentiation with respect to z.

A.2 Governing equations for the *k*-layers

Upon substitution of the above written preliminaries along with the displacement and stress assumptions formulated at Section 4.1, the RMVT assumes the following form

$$\begin{aligned}\sum_{k=1}^{N_l}\Bigg(&\int_{\Omega_k}\{\delta\boldsymbol{u}^{k^T}_\tau[(-F_\tau\boldsymbol{D}^T_p+F_\tau\boldsymbol{A}^T_p)\boldsymbol{C}_{pp}(F_s\boldsymbol{D}_p+F_s\boldsymbol{A}_p)\boldsymbol{u}^k_s\\&+(-F_\tau\boldsymbol{D}^T_p+F_\tau\boldsymbol{A}^T_p)\boldsymbol{C}_{pn}F_s\boldsymbol{\sigma}^k_{ns}+(-F_\tau\boldsymbol{D}^T_{n\Omega}+F_\tau\boldsymbol{A}^T_n\\&+F_{\tau_z})F_s\boldsymbol{\sigma}^k_{ns}]\delta\boldsymbol{\sigma}^{k^T}_\tau[(F_\tau F_s\boldsymbol{D}_{n\Omega}+F_\tau F_s\boldsymbol{A}_n+F_\tau F_{s_z}\\&-F_\tau\boldsymbol{C}_{np}(F_s\boldsymbol{D}_p+F_s\boldsymbol{A}_p))\boldsymbol{u}^k_s-F_\tau F_s\boldsymbol{C}_{nn}\boldsymbol{\sigma}^k_{ns}]\}d\Omega_k\\&+\int_{\Gamma_k}\int_{A_k}\delta\boldsymbol{u}^{k^T}_\tau[F_\tau\boldsymbol{I}^T_p\boldsymbol{C}_{pp}(F_s\boldsymbol{D}_p+F_s\boldsymbol{A}_p)\boldsymbol{u}^k_s\\&+F_\tau F_s\boldsymbol{I}^T_p\boldsymbol{C}_{pn}\boldsymbol{\sigma}^k_{ns}+F_\tau F_s\boldsymbol{I}^T_{n\Omega}\boldsymbol{\sigma}^k_{ns}]d\Gamma_k\Bigg)\\&=\sum_{k=1}^{N_l}\int_{\Omega_k}\delta\boldsymbol{u}^{k^T}_\tau\boldsymbol{p}^k_\tau d\Omega_k+\sum_{k=1}^{N_l}\int_{\Omega_k}\delta\boldsymbol{u}^{k^T}_\tau\rho^k F_\tau F_s\ddot{u}^k d\Omega_k\end{aligned} \tag{35}$$

$\boldsymbol{p}^k_\tau=\{p^k_{x\tau},p^k_{y\tau},p^k_{z\tau}\}$ are the variationally consistent load vectors coming from the applied loadings $\boldsymbol{p}^k$. Of practical interest could be the case in which both shearing ($p^k_{\alpha t}$, $p^k_{\beta t},p^k_{\alpha b},p^k_{\beta b}$) and normal ($p^k_{zt},p^k_{zb}$) surface forces are applied with correspondence to the top and or bottom surface of the layer,

$$d\Omega^p_k=d\Omega^t_k=\left(1+\frac{h_k}{2R^k_\alpha}\right)\left(1+\frac{h_k}{2R^k_\beta}\right)d\Omega_k$$

and

$$d\Omega^p_k=d\Omega^b_k=\left(1-\frac{h_k}{2R^k_\alpha}\right)\left(1-\frac{h_k}{2R^k_\beta}\right)d\Omega_k.$$

By imposing the definition of virtual variations for the unknown stress and displacement variables, the differential system of governing equations and related boundary conditions for the N_l k-layers in each Ω_k domain are found. The equilibrium and compatibility equations are

$$\delta\boldsymbol{u}^k_\tau:\ \boldsymbol{K}^{k\tau s}_{uu}\boldsymbol{u}^k_s+\boldsymbol{K}^{k\tau s}_{u\sigma}\boldsymbol{\sigma}^k_{ns}=\boldsymbol{M}^{k\tau s}\ddot{\boldsymbol{u}}^k_s+\boldsymbol{p}^k_\tau$$
$$\delta\boldsymbol{\sigma}^k_{n\tau}:\ \boldsymbol{K}^{k\tau s}_{\sigma u}\boldsymbol{u}^k_s+\boldsymbol{K}^{k\tau s}_{\sigma\sigma}\boldsymbol{\sigma}^k_{ns}=0 \tag{36}$$

with boundary conditions

$$\textit{geometrical on } \Gamma^g_k \quad \textit{mechanical on } \Gamma^m_k$$
$$\boldsymbol{u}^k_\tau=\overline{\boldsymbol{u}}^k_\tau \quad \text{or} \quad \Pi^{k\tau s}_u\boldsymbol{u}^k_s+\Pi^{k\tau s}_\sigma\boldsymbol{\sigma}^k_{ns}=\Pi^{k\tau s}_u\overline{\boldsymbol{u}}^k_s+\boldsymbol{\Pi}^{k\tau s}_\sigma\overline{\boldsymbol{\sigma}}^k_{ns} \tag{37}$$

in which the bar denotes assigned values. The introduced differential arrays are given by the following relations,

$$\boldsymbol{K}_{uu}^{k\tau s}=\int_{A_k}(-F_\tau\boldsymbol{D}_p^T+F_\tau\boldsymbol{A}_p^T)\boldsymbol{C}_{pp}^k(F_s\boldsymbol{D}_p+F_s\boldsymbol{A}_p)H_\alpha^kH_\beta^kdz_k$$

$$\boldsymbol{K}_{u\sigma}^{k\tau s}=\int_{A_k}[(-F_\tau\boldsymbol{D}_p^T+F_\tau\boldsymbol{A}_p^T)\boldsymbol{C}_{pn}^kF_s+F_{\tau_z}F_s\boldsymbol{I}+F_\tau F_s\boldsymbol{A}_n - F_\tau F_s\boldsymbol{D}_{n\Omega}^T]H_\alpha^kH_\beta^kdz_k$$

$$\boldsymbol{K}_{\sigma u}^{k\tau s}=\int_{A_k}\{F_\tau F_s\boldsymbol{D}_{n\Omega}+F_\tau F_s\boldsymbol{A}_n+F_\tau F_{s_z}\boldsymbol{I}-\boldsymbol{C}_{np}^{k\tau s}(F_\tau F_s\boldsymbol{D}_p + F_\tau F_s\boldsymbol{A}_p)\}H_\alpha^kH_\beta^kdz_k$$

$$\boldsymbol{K}_{\sigma\sigma}^{k\tau s}=-\int_{A_k}F_\tau F_s\boldsymbol{C}_{nn}^{k\tau s}H_\alpha^kH_\beta^kdz_k$$

$$\boldsymbol{\Pi}_u^{k\tau s}=\int_{A_k}F_\tau\boldsymbol{I}_p^T\boldsymbol{C}_{pp}(F_s\boldsymbol{D}_p+F_s\boldsymbol{A}_p)\boldsymbol{I}_p^TH_\alpha^kH_\beta^kdz_k$$

$$\boldsymbol{\Pi}_\sigma^{k\tau s}=\int_{A_k}(F_\tau F_s\boldsymbol{I}_p^T\boldsymbol{C}_{pn}+F_\tau F_s\boldsymbol{I}_{n\Omega}^T)H_\alpha^k;H_\beta^kdz_k$$

$$\boldsymbol{M}^{k\tau s}=\int_{A_k}\rho^kF_\tau F_s\boldsymbol{I}H_\alpha^kH_\beta^kdz_k \tag{38}$$

$\boldsymbol{I}$ is the unit array. As usual in two-dimensional modelings, the integration in the thickness direction can be first made by introducing the following layer-integrals:

$$(J^{k\tau s},J_\alpha^{k\tau s},J_\beta^{k\tau s},J_{\alpha/\beta}^{k\tau s},J_{\beta/\alpha}^{k\tau s},J_{\alpha\beta}^{k\tau s})=\int_{A_k}F_\tau F_s\left(1,H_\alpha^k,H_\beta^k,\frac{H_\alpha^k}{H_\beta^k},\frac{H_\beta^k}{H_\alpha^k},H_\alpha^kH_\beta^k\right)dz$$

$$J_{\alpha\beta}^{k\tau_z s}=\int_{A_k}F_{\tau_z}F_sH_\alpha^kH_\beta^kdz,\quad J_{\alpha\beta}^{k\tau s_z}=\int_{A_k}F_\tau F_{s_z}H_\alpha^kH_\beta^kdz \tag{39}$$

As a further step, the differential and algebraic operators can be conveniently split into the two terms related to the H_α^k and H_β^k, respectively,

$$(\boldsymbol{D}_p,\boldsymbol{A}_p,\boldsymbol{D}_{n\Omega},\boldsymbol{A}_n,\boldsymbol{I}_p,\boldsymbol{I}_{n\Omega})=\frac{1}{H_\alpha}(\boldsymbol{D}_p^\alpha,\boldsymbol{A}_p^\alpha,\boldsymbol{D}_{n\Omega}^\alpha,\boldsymbol{A}_n^\alpha,\boldsymbol{I}_p,\boldsymbol{I}_{n\Omega}) + \frac{1}{H_\beta}(\boldsymbol{D}_p^\beta,\boldsymbol{A}_p^\beta,\boldsymbol{D}_{n\Omega}^\beta,\boldsymbol{A}_n^\beta,\boldsymbol{I}_p^\beta,\boldsymbol{I}_{n\Omega}^\beta) \tag{40}$$

Therefore, the differential operators of Eq. (38) are written

$$\boldsymbol{K}_{uu}^{k\tau s}=(-\boldsymbol{D}_p^{\alpha T}+\boldsymbol{A}_p^{\alpha T})\boldsymbol{C}_{pp}[J_{\beta/\alpha}^{k\tau s}(\boldsymbol{D}_p^\alpha+\boldsymbol{A}_p^\alpha)+J^{k\tau s}(\boldsymbol{D}_p^\beta+\boldsymbol{A}_p^\beta)] + (-\boldsymbol{D}_p^{\beta T}+\boldsymbol{A}_p^{\beta T})\boldsymbol{C}_{pp}[J_{\alpha/\beta}^{k\tau s}(\boldsymbol{D}_p^\alpha+\boldsymbol{A}_p^\alpha) + J^{k\tau s}(\boldsymbol{D}_p^\beta+\boldsymbol{A}_p^\beta)]$$

$$\boldsymbol{K}_{u\sigma}^{k\tau s}=(-J_\beta^{k\tau s}\boldsymbol{D}_p^{\alpha T}-J_\alpha^{k\tau s}\boldsymbol{D}_p^{\beta T}+J_\alpha^{k\tau s}\boldsymbol{A}_p^{\beta T}+J_\beta^{k\tau s}\boldsymbol{A}_p^{\alpha T})\boldsymbol{C}_{pn}^k + J_{\alpha\beta}^{k\tau_z s}\boldsymbol{I}+(J_\beta^{k\tau s}\boldsymbol{A}_n^{\alpha T}+J_\alpha^{k\tau s}\boldsymbol{A}_n^{\beta T})-J_\beta^{k\tau s}\boldsymbol{D}_{n\Omega}^{\alpha T}-J_\alpha^{k\tau s}\boldsymbol{D}_{n\Omega}^{\beta T}$$

$$\boldsymbol{K}_{\sigma u}^{k\tau s}=-\boldsymbol{C}_{np}^k(J_\beta^{k\tau s}\boldsymbol{D}_p^\alpha+J_\alpha^{k\tau s}\boldsymbol{D}_p^\beta+J_\alpha^{k\tau s}\boldsymbol{A}_p^\beta+J_\beta^{k\tau s}\boldsymbol{A}_p^\alpha)+J_{\alpha\beta}^{k\tau s_z}\boldsymbol{I} + (J_\beta^{k\tau s}\boldsymbol{A}_n^\alpha+J_\alpha^{k\tau s}\boldsymbol{A}_n^\beta)+J_\beta^{k\tau s}\boldsymbol{D}_{n\Omega}^\alpha+J_\alpha^{k\tau s}\boldsymbol{D}_{n\Omega}^\beta$$

$$\boldsymbol{K}_{\sigma\sigma}^{k\tau s}=-J_{\alpha\beta}^{k\tau s}\boldsymbol{C}_{nn}^{k\tau s}$$

$$\boldsymbol{\Pi}_u^{k\tau s}=(J_{\beta/\alpha}^{k\tau s}\boldsymbol{I}_p^{\alpha T}+J^{k\tau s}\boldsymbol{I}_p^{\beta T})\boldsymbol{C}_{pp}(\boldsymbol{D}_p^\alpha+\boldsymbol{A}_p^\alpha)+(J^{k\tau s}\boldsymbol{I}_p^{\alpha T} + J_{\alpha/\beta}^{k\tau s}\boldsymbol{I}_p^{\beta T})\boldsymbol{C}_{pp}(\boldsymbol{D}_p^\beta+\boldsymbol{A}_p^\beta)$$

$$\boldsymbol{\Pi}_\sigma^{k\tau s}=(J_\beta^{k\tau s}\boldsymbol{I}_p^{\alpha T}+J_\alpha^{k\tau s}\boldsymbol{I}_p^{\beta T})\boldsymbol{C}_{pn}+J_\beta^{k\tau s}\boldsymbol{I}_{n\Omega}^{\alpha T}+J_\alpha^{k\tau s}\boldsymbol{I}_{n\Omega}^{\beta T} \tag{41}$$

The inertia array is found

$$\boldsymbol{M}_{ij}^{k\tau s}=J_{\alpha\beta}^{k\tau s}\delta_{ij},\quad i,j=1,3 \tag{42}$$

where the Kroneker symbol δ_{ij} has been introduced. Cylindrical shell equations are simply obtained by enforcing $R_\alpha=\infty$ (or $R_\beta=\infty$) while spherical shell geometries correspond to the case $R_\alpha=R_\beta$. Neglecting all the curvature terms, the governing equations written for multilayer plates are obtained. Explicit forms of the governing equations for each layer can be written by expanding the introduced subscripts and superscripts in the previous arrays as follows

$$k=1,2,\ldots,N_l;\quad \tau=t,r,b,\quad s=t,r,b,\quad (r=2,\ldots,N)$$

Governing equations related to Layer-Wise as well as Equivalent Single Layer related to different order of the expansion of displacement and stress models can be implemented. The shell equations reported by Jing and Tzeng [78], Bhaskar and Varadan [115] as well as the plate equations by Murakami [44] and Toledano and Murakami [45,46] can be obtained as particular cases.

A.3 Governing equations at multilayer level

In the previous section, the governing equations have been written for the N_l-layers, which have been considered to be independent. Multilayer equations can be written according to the usual variational statements: stiffness and/or compliances related to the same variables are accumulated in this process. Interlaminar continuity conditions, eg, C_z^0-Requirements, are imposed at this stage. An example is given in Fig. 16. It is clear in this figure that the choice of using interface values as unknown variables permits one to impose C_z^0-Requirements and to obtain multilayered matrices in a simple manner, ie, simply by shifting the layer-matrices along the diagonal of the multilayered matrix. Details on this procedure can be found in the already mentioned author's papers. Multilayer arrays are obtained at the very end of this assemblage procedure. In compact form the equilibrium and constitutive equations are

$$\boldsymbol{K}_{uu}\boldsymbol{u}+\boldsymbol{K}_{u\sigma}\boldsymbol{\sigma}_n=\boldsymbol{M}\ddot{\boldsymbol{u}}+\boldsymbol{p}+\boldsymbol{p}_u^{1N_l}$$

$$\boldsymbol{K}_{\sigma u}\boldsymbol{u}+\boldsymbol{K}_{\sigma\sigma}\boldsymbol{\sigma}_n=\boldsymbol{p}_\sigma^{1N_l} \tag{43}$$

while the boundary conditions are

$$\boldsymbol{u}=\overline{\boldsymbol{u}}\ \text{ or }\ \boldsymbol{\Pi}_u\boldsymbol{u}+\boldsymbol{\Pi}_\sigma\boldsymbol{\sigma}_n=\boldsymbol{\Pi}_u\overline{\boldsymbol{u}}+\boldsymbol{\Pi}_\sigma\overline{\boldsymbol{\sigma}}_n+\boldsymbol{q}_\sigma^{1N_l} \tag{44}$$

$\boldsymbol{p}_u^{1N_l}$ and $\boldsymbol{p}_\sigma^{1N_l}$ are the arrays obtained from the transverse stress values imposed at the top/bottom of the plate.

APPENDIX B MULTILAYER PLATE FINITE ELEMENTS

This appendix shows how the RMVT can be applied to derive finite element matrices of a multilayer plate in the static case.

B.1 Preliminary

Geometry and notations of a multilayer plate are those reported in Fig. 4: *x*, *y*, *z* is a system of Cartesian coordinates; *z* is the thickness coordinate. As stated in Section 4.4.2, finite element approximations for $\boldsymbol{u}_\tau^k$ and $\boldsymbol{\sigma}_{n\tau}^k$ are in fact now expressed in terms of related nodal unknowns by means of shape functions. For the sake of simplicity, the shape functions are similarly selected for stresses and displacements,

$$\mathbf{u}_\tau^k = R_i \mathbf{q}_{\tau i}^k \quad (i=1,2,\ldots,N_n) \tag{45}$$

$$\boldsymbol{\sigma}_{n\tau}^k = R_i \mathbf{g}_{\tau i}^k \quad (i=1,2,\ldots,N_n) \tag{46}$$

where

$$\mathbf{q}_{\tau i}^k = [q_{u_x\tau i}^k, q_{u_y\tau i}^k, q_{u_z\tau i}^k], \quad \mathbf{g}_{\tau i}^k = [g_{u_x\tau i}^k, g_{u_y\tau i}^k, g_{u_z\tau i}^k] \tag{47}$$

$\mathbf{q}_{\tau i}^k$ and $\mathbf{g}_{\tau i}^k$ are the nodal displacements and stress variables. N_n is the number of the nodes in the element and R_i are the related shape functions. Strain displacement relations in the linear case and in rectangular coordinates are:

$$\varepsilon_p^k = F_\tau \boldsymbol{D}_p(R_i \boldsymbol{I}) \mathbf{q}_{\tau i}^k \tag{48}$$

$$\varepsilon_n^k = F_\tau \boldsymbol{D}_{n\Omega}(R_i \boldsymbol{I}) \mathbf{q}_{\tau i}^k + F_{\tau,z} R_i \mathbf{q}_{\tau i}^k \tag{49}$$

where

$$\boldsymbol{D}_p = \begin{bmatrix} \partial_x & 0 & 0 \\ 0 & \partial_y & 0 \\ \partial_x & \partial_x & 0 \end{bmatrix}, \quad \boldsymbol{D}_{n\Omega} = \begin{bmatrix} 0 & 0 & \partial_x \\ 0 & 0 & \partial_y \\ 0 & 0 & 0 \end{bmatrix}.$$

B.2 Finite element matrices

Upon substitution of previous written relations, the RMVT leads to

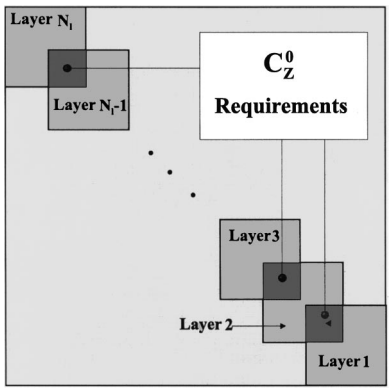

Fig. 16 An example showing how C_z^0-Requirements are imposed

$$\int_\Omega \{ \delta \mathbf{q}_{\tau i}^{kT} [\boldsymbol{D}_p^T(R_i \boldsymbol{I}) \mathbf{Z}_{pp}^{k\tau s} \boldsymbol{D}_p(R_j \boldsymbol{I})] \mathbf{q}_{sj}^k + \delta \mathbf{q}_{\tau i}^{kT} [\boldsymbol{D}_p^T(R_i \boldsymbol{I}) \mathbf{Z}_{pn}^{k\tau s} R_j] \mathbf{g}_{sj}^k + \delta \mathbf{q}_{\tau i}^{kT} [\boldsymbol{D}_{n\Omega}^T(R_i \boldsymbol{I}) E_{\tau s} R_j + E_{\tau,z^s} R_i R_j \boldsymbol{I}] \mathbf{g}_{sj}^k + \delta \mathbf{g}_{\tau i}^{kT} [R_i E_{\tau s} \boldsymbol{D}_{n\Omega}(R_j \boldsymbol{I}) + E_{\tau s,z} R_i R_j \boldsymbol{I}] \mathbf{q}_{sj}^k + \delta \mathbf{g}_{\tau i}^{kT} [R_i \mathbf{Z}_{np}^{k\tau s} \boldsymbol{D}_p(R_j \boldsymbol{I})] \mathbf{q}_{sj}^k + \delta \mathbf{g}_{\tau i}^{kT} [R_i \mathbf{Z}_{nn}^{k\tau s} N_j] \mathbf{g}_{sj}^k d\Omega = \delta L_e \tag{50}$$

where

$$(\mathbf{Z}_{pp}^{k\tau s}, \mathbf{Z}_{pn}^{k\tau s}, \mathbf{Z}_{np}^{k\tau s}, \mathbf{Z}_{nn}^{k\tau s}) = (\boldsymbol{C}_{pp}^k, \boldsymbol{C}_{pn}^k, \boldsymbol{C}_{np}^k, \boldsymbol{C}_{nn}^k) E_{\tau s}$$

Equation (50) can also be written

$$\delta \mathbf{q}_{\tau i}^{kT} [\boldsymbol{K}_{uu}^{k\tau sij} \mathbf{q}_{sj}^k + \boldsymbol{K}_{u\sigma}^{k\tau sij} \mathbf{g}_{sj}^k] + \delta \mathbf{g}_{\tau i}^{kT} [\boldsymbol{K}_{\sigma u}^{k\tau sij} \mathbf{q}_{sj}^k + \boldsymbol{K}_{\sigma\sigma}^{k\tau sij} \mathbf{g}_{sj}^k] = \delta \mathbf{q}_{\tau i}^{kT} \boldsymbol{P}_{\tau i}^k \tag{51}$$

where the following definitions have been introduced,

$$\boldsymbol{K}_{uu}^{k\tau sij} = \int_\Omega [\boldsymbol{D}_p^T(R_i \boldsymbol{I}) \mathbf{Z}_{pp}^{k\tau s} \boldsymbol{D}_p(R_j \boldsymbol{I})] d\Omega$$

$$\boldsymbol{K}_{u\sigma}^{k\tau sij} = \int_\Omega [\boldsymbol{D}_p^T(R_i \boldsymbol{I}) \mathbf{Z}_{pn}^{k\tau s} R_j + \boldsymbol{D}_{n\Omega}^T(R_i \boldsymbol{I}) E_{\tau s} R_j + E_{\tau,z^s} R_i R_j \boldsymbol{I}] d\Omega$$

$$\boldsymbol{K}_{\sigma u}^{k\tau sij} = \int_\Omega [R_i E_{\tau s} \boldsymbol{D}_{n\Omega}(R_j \boldsymbol{I}) + E_{\tau s,z} R_i R_j \boldsymbol{I} - R_i \mathbf{Z}_{np}^{k\tau s} \boldsymbol{D}_p(R_j \boldsymbol{I})] d\Omega$$

$$\boldsymbol{K}_{\sigma\sigma}^{k\tau sij} = \int_\Omega [-R_i \mathbf{Z}_{nn}^{k\tau s} R_j] d\Omega \tag{52}$$

The nodal loadings related to the external loadings have been introduced. In compact form, equilibrium and compatibility equations are:

$$\delta \mathbf{q}_{\tau i}^{kT}: \quad \boldsymbol{K}_{uu}^{k\tau sij} \mathbf{q}_{sj}^k + \boldsymbol{K}_{u\sigma}^{k\tau sij} \mathbf{g}_{sj}^k = \mathbf{P}_{\tau i}^k$$

$$\delta \mathbf{g}_{\tau i}^{kT}: \quad \boldsymbol{K}_{\sigma u}^{k\tau sij} \mathbf{q}_{sj}^k + \boldsymbol{K}_{\sigma\sigma}^{k\tau sij} \mathbf{g}_{sj}^k = \mathbf{0} \tag{53}$$

These equations have been written for each *k*-layer. Multilayer plate element equations are built by imposing the C_z^0-Requirements. Assembly from elements to structural level are made as usual in finite element technique. Stress variables can be treated as described in Section 4.4.3.

REFERENCES

[1] Reissner E (1984), On a certain mixed variational theory and a proposed application, *Int. J. Numer. Methods Eng.* **20**, 1366–1368.
[2] Reissner E (1986a), On a mixed variational theorem and on a shear deformable plate theory, *Int. J. Numer. Methods Eng.* **23**, 193–198.
[3] Reissner E (1986b) On a certain mixed variational theorem and on laminated elastic shell theory, *Proc of Euromech-Colloquium* **219**, 17–27.
[4] Hildebrand FB, Reissner E, and Thomas GB (1938), Notes on the foundations of the theory of small displacements of orthotropic shells, NACA TN-1833, Washington DC.
[5] Reissner E (1952), Stress strain relation in the theory of thin elastic shell, *J. Math. Phys.* **31**, 109–119.
[6] Reissner E (1964), On the form of variationally derived shell equations, *ASME J. Appl. Mech.* **31**, 233–328.
[7] Carrera E (1995), A class of two-dimensional theories for anisotropic

multilayered plates analysis, Accademia delle Scienze di Torino, Memorie Scienze Fisiche, 19–20 (1995–1996), 1–39.
[8] Carrera E (1997c), C_z^0 Requirements-Models for the two dimensional analysis of multilayered structures, *Compos. Struct.* **37**, 373–384.
[9] Koiter WT (1959), A consistent first approximations in the general theory of thin elastic shells, *Proc. of Symp. on the Theory of Thin Elastic Shells*, Aug, North-Holland, Amsterdam, 12–23.
[10] Cauchy AL (1828), Sur l'equilibre et le mouvement d'une plaque solide, *Exercises de Matematique* **3**, 328–355.
[11] Poisson SD (1829), Memoire sur l'equilibre et le mouvement des corps elastique, *Mem. Acad. Sci.* **8**, 357.
[12] Kirchhoff G (1850), Uber das Gleichgewicht und die Bewegung einer elastishen Scheibe, *J. Angew Math.* **40**, 51–88.
[13] Love AEH (1927), *The Mathematical Theory of Elasticity*, 4th Edition, Cambridge Univ Press, Cambridge.
[14] Cicala P (1959), Sulla teoria elastica della parete sottile, *Giornale del Genio Civile, fascicoli* **6e**, 9.
[15] Cicala P (1965), *Systematic Approach to Linear Shell Theory*, Levrotto and Bella, Torino.
[16] Goldenveizer AL (1961), *Theory of Thin Elastic Shells*, Int. Series of Monograph in Aeronautics and Astronautics, Pergamon Press, New York.
[17] Jones RM (1975), *Mechanics of Composite Materials*, Mc Graw-Hill, New York.
[18] Reissner E (1945), The effect of transverse shear deformation on the bending of elastic plates, *ASME J. Appl. Mech.* **12**, 69–76.
[19] Mindlin RD (1951), Influence of rotatory inertia and shear in flexural motions of isotropic elastic plates, *ASME J. Appl. Mech.* **18**, 1031–1036.
[20] Whitney JM (1969), The effects of transverse shear deformation on the bending of laminated plates, *J. Compos. Mater.* **3**, 534–547.
[21] Reddy JN (1997), *Mechanics of Laminated Composite Plates, Theory and Analysis*, CRC Press.
[22] Sun CT and Whitney JM (1973), On the theories for the dynamic response of laminated plates, *AIAA J.* **11**, 372–398.
[23] Lo KH, Christensen RM, and Wu EM (1977), A higher-order theory of plate deformation, Part 2: Laminated plates, *ASME J. Appl. Mech.* **44**, 669–676.
[24] Librescu L (1975), *Elasto-Statics and Kinetics of Anisotropic and Heterogeneous Shell-Type Structures*, Noordhoff Int, Leyden, Netherland.
[25] Vlasov BF (1957), On the equations of Bending of plates, *Dokl. Akad. Nauk Arm. SSR* , **3**, 955–979.
[26] Reddy JN (1984b), A simple higher order theories for laminated composites plates, *AMSE J. Appl. Mech.* **52**, 745–742.
[27] Reddy JN and Phan ND (1985), Stability and vibration of isotropic, orthotropic, and laminated plates according to a higher order shear deformation theory, *J. Sound Vib.* **98**, 157–170.
[28] Srinivas S (1973), A refined analysis of composite laminates, *J. Sound Vib.* **30**, 495–507.
[29] Cho KN, Bert CW, and Striz AG (1991), Free vibrations of laminated rectangular plates analyzed by higher-order individual-Layer theory, *J. Sound Vib.* **145**, 429–442.
[30] Barbero EJ, Reddy JN, and Teply JL (1990), General two-dimensional theory of laminated cylindrical shells, *AIAA J.* **28**, 544–553.
[31] Nosier A, Kapania RK, and Reddy JN (1993), Free vibtation analysis of laminated plates using a layer-wise theory, *AIAA J.* **31**, 2335–2346.
[32] Pagano NJ (1969), Exact solutions for composite laminates in cylindrical bending, *J. Compos. Mater.* **3**, 398–411.
[33] Lekhnitskii SG (1935), Strength calculation of composite beams, *Vestn. inzhen. i tekhnikov* **9**, 540-544.
[34] Lekhnitskii SG (1968), *Anisotropic Plates*, 2nd Edition, Translated from the 2nd Russian Edition by SW Tsai, Cheron, Bordon, and Breach.
[35] Ambartsumian SA (1969), *Theory of Anisotropic Plates*, Translated from Russian by T Cheron and Edited by JE Ashton Tech. Pub. Co.
[36] Grigolyuk EI and Kulikov GM (1988), General directions of the development of theory of shells, *Mekh. Kompoz. Mater.* **24**, 287–298.
[37] Ren JG (1987), Exact solutions for laminated cylindrical shells in cylindrical bending, *Compos. Sci. Technol.* **29**, 169–187.
[38] Rath BK and Das YC (1973), Vibration of layered shells, *J. Sound Vib.* **28**, 737–757.
[39] Aitharaju VR and Averill RC (1999), C^0 zig-zag kinematic displacement models for the analysis of laminated composites, *Mech. Compos. Mater. Struct.* **6**, 31–56.
[40] Reddy JN (1984a), *Energy and Variational Methods in Applied Mechanics*, John Wiley, NY.
[41] Atluri SN, Tong P, and Murakawa H (1983), Recent studies in hybrid and mixed finite element methods in mechanics, in *Hybrid and Mixed Finite Element Methods*, Edited by SN Atluri RH Gallagher, and O Zienkiewicz, John Wiley and Sons, 51–71.
[42] Murakami H (1984), A laminated beam theory with interlayer slip, *ASME J. Appl. Mech.* **51**, 551–559.
[43] Murakami H (1985), Laminated composite plate theory with improved in-plane responses, *ASME Proc. of PVP Conf, New Orleans* **98-2**, 257–263.
[44] Murakami H (1986), Laminated composite plate theory with improved in-plane responses, *ASME J. Appl. Mech.* **53**, 661–666.
[45] Toledano A and Murakami H (1987a), A high-order laminated plate theory with improved in-plane responses, *Int. J. Solids Struct.* **23**, 111–131.
[46] Toledano A and Murakami H (1987b), A composite plate theory for arbitrary laminate configurations, *ASME J. Appl. Mech.* **54**, 181–189.
[47] Librescu L and Reddy JN (1986), A critical review and generalization of transverse shear deformable anisotropic plates, *Euromech Colloquium 219, Kassel, Sept, 1986 Refined Dynamical Theories of Beams, Plates and Shells and their Applications*, Elishakoff and Irretier (eds), Springer Verlag, Berlin, 32–43.
[48] Kapania RK (1989), A review on the analysis of laminated shells, *J. Pressure Vessel Technol.* **111**, 88–96.
[49] Kapania RK and Raciti S (1989), Recent advances in analysis of laminated beams and plates, *AIAA J.* **27**, 923–946.
[50] Noor AK and Burton WS (1989b), Assessment of shear deformation theories for multilayered composite plates, *Appl. Mech. Rev.* **42** (1), 1–13.
[51] Noor AK and Burton WS (1990), Assessment of computational models for multilayered composite shells, *Appl. Mech. Rev.* **43** (4), 67–97.
[52] Reddy JN and Robbins DH (1994), Theories and computational models for composite laminates, *Appl. Mech. Rev.* **47** (6), 147–165.
[53] Soldatos KP and Timarch T (1993), A unified formulation of laminated composites, shear deformable, five-degrees-of-freedom cylindrical shell theories, *Composite Structures* **25**, 165–171.
[54] Noor AK, Burton S, and Bert CW (1996), Computational model for sandwich panels and shells, *Appl. Mech. Rev.* **49**(3), 155–199.
[55] Washizu K (1968), *Variational Method in Elasticity and Plasticity*, Oxford, Pergamon Press.
[56] Antona E (1991), Mathematical model and their use in engineering, *Applied Mathematics in the Aerospace Science/Engineering*, by A Miele and A Salvetti (eds), vol 44, 395–433.
[57] Zienkiewicz OC (1986), *The Finite Element Method*, Mc Graw-Hill, London.
[58] Carrera E (1998d), Layer-wise mixed models for acurate vibration analysis of multilayered plates, *ASME J. Appl. Mech.* **65**, 820–828.
[59] Carrera E (1999a), Multilayered shell theories that account for a layer-wise mixed description, Part I. Governing equations, *AIAA J.* **37**(9), 1107–1116.
[60] Carrera E (1999b), Multilayered shell theories that account for a layer-wise mixed description, Part II. Numerical evaluations, *AIAA J.* **37**(9), 1117–1124.
[61] Carrera E (1999c), A Reissner's mixed variational theorem applied to vibration analysis of multilayered shells, *ASME J. Appl. Mech.* **66**, 69–78.
[62] Rao KM and Meyer-Piening HR (1990), Analysis of thick laminated anisotropic composites plates by the finite element method, *Compos. Struct.* **15**, 185–213.
[63] Messina A (2001), Two generalized higher order theories in free vibration studies of multilayered plates, *J. Sound Vib.* **242**, 125–150.
[64] Carrera E (1996), C^0 Reissner-Mindlin multilayered plate elements including zig-zag and interlaminar stresses continuity, *Int. J. Numer. Methods Eng.* **39**, 1797–1820.
[65] Murakami H and Yamakawa J (1996), Dynamic response of plane anisotropic beams with shear deformation, *ASCE J. Eng. Mech.* **123**, 1268–1275.
[66] Murakami H, Reissner E, and Yamakawa J (1996), Anisotropic beam theories with shear deformation, *ASME J. Appl. Mech.* **63**, 660–668.
[67] Soldatos KP (1987), Cylindrical bending of Cross-ply Laminated Plates: Refined 2D Plate theories in comparison with the Exact 3D elasticity solution, Tech Report No. 140, Dept. of Math., University of Ioannina, Greece.
[68] Carrera E (1998a), A refined multilayered finite element model applied to linear and nonlinear analysis of sandwich structures, *Compos. Sci. Technol.* **58**, 1553–1569.
[69] Carrera E (1998b), Mixed layer-wise models for multilayered plates analysis, *Compos. Struct.* **43**, 57–70.
[70] Carrera E (1998c), Evaluation of layer-wise mixed theories for laminated plates analysis, *AIAA J.* **26**, 830–839.

[71] Carrera E (1999d), Transverse normal stress effects in multilayered plates, *ASME J. Appl. Mech.* **66**, 1004–1012.
[72] Carrera E (1999e), A study of transverse normal stress effects on vibration of multilayered plates and shells, *J. Sound Vib.* **225**, 803–829.
[73] Carrera E (2000a), Single-layer *vs* multi-layers plate modelings on the basis of Reissner's mixed theorem, *AIAA J.* **38**, 342–343.
[74] Carrera E (2000b), A priori vs a posteriori evaluation of transverse stresses in multilayered orthotropic plates, *Compos. Struct*, **48**, 245–260.
[75] Carrera E (2000c), An assessment of mixed and classical theories for thermal stress analysis of orthotropic plates, *J. Therm. Stresses* **23**, 797–831.
[76] Bhaskar K and Varadan TK (1991), A higher-order theory for bending analysis of laminated shells of revolution, *Comput. Struct.* **40**, 815–819.
[77] Jing H and Tzeng KG (1993a), On two mixed variational principles for thick laminated composite plates, *Compos. Struct.*
[78] Jing H and Tzeng KG (1993b), Refined shear deformation theory of laminated shells, *AIAA J.* **31**, 765–773.
[79] Jing H and Liao ML (1989), Partial hybrid stress element for the analysis of thick laminate composite plates, *Int. J. Numer. Methods Eng.* **28**, 2813–2827.
[80] Toledano A and Murakami H (1987c), A high-order mixture model for periodic particulate composites *Int. J. Solids Struct.* **23**, 989–1002.
[81] Carrera E and Kröplin B (1997), Zig-Zag and interlaminar equilibria effects in large deflection and postbuckling analysis of multilayered plates, *Mech. Compos. Mater. Struct.* **4**, 69–94.
[82] Carrera E and Krause H (1998b), An investigation on nonlinear dynamics of multilayered plates accounting for C_z^0 requirements, *Comput. Struct.* **69**, 463–486.
[83] Carrera E (1997b), An improved Reissner-Mindlin-Type model for the electromechanical analysis of multilayered plates including piezo-layers, *J. Intell. Mater. Syst. Struct.* **8**, 232–248.
[84] Carrera E and Niglia F (1998), A refined multilayered FEM model applied to sandwich structures, *Mechanics of Sandwich Structures*, A Vautrin (ed), Kluwer Academic Publ, 61–69.
[85] Carrera E and Parisch H (1998a), Evaluation of geometrical nonlinear effects of thin and moderately thick multilayered composite shells, *Compos. Struct.* **40**, 11–24.
[86] Brank B and Carrera E (2000a), A family of shear-deformable shell finite elements for composite structures, *Comput. Struct.* **76**, 297–297.
[87] Brank B and Carrera E (2000b), Multilayered shell finite element with interlaminar continuous shear stresses: A refinement of the Reissner-Mindlin formulation, *Int. J. Numer. Methods Eng.* **48**, 843–874.
[88] Carrera E and Demasi L, Multilayered finite plate element based on Reissner Mixed Variational Theorem. Part I: Theory; Part II: Numerical analysis, to appear.
[89] Carrera E and Demasi L (2000b), An assessment of multilayered finite plate element in view of the fulfillment of the C_z^0-Requirements, *AIMETA GIMC Conf*, Brescia, Nov, 340–348
[90] Carrera E and Demasi L (2000c), Sandwich plate analysis by finite plate element and Reissner Mixed Theorem, *V Int. Conf. on Sandwich Construction*, Zurich, Sept, vol I, 301–312
[91] Latham C, Toledano A, Murakami H, and Seible F (1988), A shear deformable two-layer plate element with interlayer slip, *Int. J. Numer. Methods Eng.* **26**, 1769–1789.
[92] Toledano A and Murakami H (1988), A shear-deformable two-layer plate theory with interlayer slip, *ASCE J. Eng. Mech.* **114**(4), 604–623.
[93] Hegemier GA, Murakami H, and Hageman LJ (1985), On tension stiffening in reinforced concrete, *Mech. Mater.* **4**(2), 161–179.
[94] Murakami H and Hegemier GA (1986a), On simulating steel-concrete interaction in reinforced concrete, Part I: Theoretical development, *Mech. Mater.* **5**, 171–185.
[95] Murakami H and Hegemier GA (1986b), A mixture model for unidirectionally fiber-reinforced composites, *ASME J. Appl. Mech.* **53**(4), 765–773.
[96] Murakami H and Hegemier GA (1989), Development of a nonlinear continuum model for wave propagation in jointed media: theory for single joint set, *Mech. Mater.* **8**, 199–218.
[97] Murakami H and Toledano A (1990), A high-order mixture homogenization of bi-laminated composites, *ASME J. Appl. Mech.* **57**, 388–397.
[98] Toledano A and Murakami H (1991), High-order mixture homogenization of fiber-reinforced composites, *ASME J. Energy Resour. Technol.* **113**, 254–263.
[99] Murakami H, Impelluso TJ, and Hegemier GA (1991), A continuum finite element for single-set jointed media *Int. J. Numer. Methods Eng.* **31**, 1169–1194.
[100] Impelluso TJ and Murakami H (1995), A homogenized continuum model for fiber-reinforced composites, *Z. Angew. Math. Mech.* **75** (3), 171–188.
[101] Noor AK and Burton WS (1989a), Stress and free vibration analyses of multilayered composite plates, *Compos. Structu.* **11**, 183–204.
[102] Cho M and Parmerter RR (1993), Efficient higher order composite plate theory for general lamination configurations, *AIAA J.* **31**, 1299–1305.
[103] Idlbi A, Karama M, and Touratier M (1997), Comparison of various laminated plate theories, *Compos. Struct.* **37**, 173–184.
[104] Ren JG (1986), A new theory for laminated plates, *Compos. Sci. Technol.* **26**, 225–239.
[105] Bhaskar K, Varadan TK, and Ali JSM (1996), Thermoelastic solution for orthotropic and anisotropic composites laminates, *Composites, Part B* **27B**, 415–420.
[106] Varadan TK and Bhaskar K (1991), Bending of Laminated Orthotropic Cylindrical Shells - An Elasticity Approach, *Compos. Struct.* **17**, 141–156.
[107] Dennis ST and Palazotto AN (1991), Laminated shell in cylindrical bending, two-dimensional approach vs exact, *AIAA J.* **29**, 647–650.
[108] Ye JQ and Soldatos KP (1994), Three-dimensional vibration of laminated cylinders and cylindrical panels with symmetric or antisymmetric cross-ply lay-up, *Composites Eng.* **4**, 429–444.
[109] Timarci T and Soldatos KP (1995), Comparative dynamic studies for symmetric cross-ply circular cylindrical shells on the basis of a unified shear deformable shell theory, *J. Sound Vib.* **187**, 609–624.
[110] Dischiuva M and Carrera E (1992), Elasto-dynamic behavior of relatively thick, symmetrically laminated, anisotropic circular cylindrical shells, *ASME J. Appl. Mech.* **59**, 222–223.
[111] Liou WJ and Sun CT (1987), A three-dimensional hybrid stress isoparametric element for the analysis of laminated composite plates, *Comput. Struct.* **25**, 241–249.
[112] Moriya K (1986), Laminated plate and shell elements for finite element analysis of advanced fiber reinforced composite structure, Laminated Composite Plates, in Japanese, *Trans. Jpn. Soc. Mech. Eng.* **52**, 1600–1607.
[113] Bathe KJ and Dvorkin EN (1985), A four node plate bending element based on Mindlin/Reissner plate theory and mixed interpolation, *Int. J. Numer. Methods Eng.* **21**, 367–383.
[114] Kraus H (1967) *Thin Elastic Shells*, John Wiley, NY.
[115] Bhaskar K and Varadan TK (1992), Reissner's new mixed variational principle applied to laminated cylindrical shells, *ASME J. Pressure Vessel Technol.* **114**, 115–119.
[116] Dischiuva M (1993), A general quadrilater, multilayered plate element with continuous interlaminar stresses, *Compos. Struct.* **47**, 91–105.
[117] Kant T and Kommineni JR (1989), Large amplitude free vibration analysis of cross-ply composite and sandwich laminates with a refined theory and C^0 finite elements, *Comput. Struct.* **50**, 123–134.
[118] Pagano NJ and Hatfield SJ (1972), Elastic behavior of multilayered bidirectional composites, *AIAA J.* **10**, 931–933.
[119] Pagano NJ (1970), Exact solutions for rectangular bidirection composites and sandwich plates, *J. Compos. Mater.* **4**, 20–34.

After earning two degrees (Aeronautics, 1986 and Aerospace Engineering, 1988) in the Politecnico di Torino, **Erasmo Carrera** *received his PhD degree in Aerospace Engineering in 1991, at the Politecnico di Milano-Politecnico di Torino-Universitá di Pisa. He began working as a Researcher in the Department of Aerospace of Politecnico di Torino in 1992 holding courses on Missiles and Aerospace Structure Design, Plates and Shells, and the Finite Element Method and since 2000 is Associate Professor of Aeroelasticity. He visited twice the Institute für Statik und Dynamik, Universität Stuttgart, the first time as a PhD student (six months in 1991) and then as Visiting Scientist on a GKKS Grant (18 months in 1995–96). In the Summer of '96 he was Visiting Professor at the ESM Dept of Virginia Tech. His main research topics are: composite materials, finite elements, plates and shells, postbuckling and stability by FEM, smartstructures, aeroelasticity, multibody dynamics and design and analysis of non classical lifting systems. He is an author of more than eighty articles on these topics, many of which have been published in international journals. He serves as a referee for many journals such as AIAA Journal, Journal of Sound and Vibration and International Journal of Solids and Structures.*